ISSN 2096-7071
CN 10-1629/R1

CHINA CDC WEEKLY

Vol. 4 No. 40 Oct. 7, 2022

中国疾病预防控制中心周报

COVID-19 ISSUE (31)

ISSN 2096-7071

Vital Surveillances

Travel-related Importation and Exportation Risks of SARS-CoV-2 Omicron Variant in 367 Prefectures (Cities) — China, 2022

Yuan Bai[1,&]; Mingda Xu[2,&]; Caifen Liu[1,2]; Mingwang Shen[3]; Lin Wang[4]; Linwei Tian[1]; Suoyi Tan[5]; Lei Zhang[3]; Petter Holme[6,7]; Xin Lu[5]; Eric H. Y. Lau[1,2]; Benjamin J. Cowling[1,2,#]; Zhanwei Du[1,2]

ABSTRACT

Introduction: Minimizing the importation and exportation risks of coronavirus disease 2019 (COVID-19) is a primary concern for sustaining the "Dynamic COVID-zero" strategy in China. Risk estimation is essential for cities to conduct before relaxing border control measures.

Methods: Informed by the daily number of passengers traveling between 367 prefectures (cities) in China, this study used a stochastic metapopulation model parameterized with COVID-19 epidemic characteristics to estimate the importation and exportation risks.

Results: Under the transmission scenario (R_0=5.49), this study estimated the cumulative case incidence of Changchun City, Jilin Province as 3,233 (95% confidence interval: 1,480, 4,986) before a lockdown on March 14, 2022, which is close to the 3,168 cases reported in real life by March 16, 2022. In a total of 367 prefectures (cities), 127 (35%) had high exportation risks according to the simulation and could transmit the disease to 50% of all other regions within a period from 17 to 94 days. The average time until a new infection arrives in a location in 1 of the 367 prefectures (cities) ranged from 26 to 101 days.

Conclusions: Estimating COVID-19 importation and exportation risks is necessary for preparedness, prevention, and control measures of COVID-19 — especially when new variants emerge.

The ongoing global pandemic of coronavirus disease 2019 (COVID-19) caused by severe acute respiratory syndrome coronavirus 2 (SARS-CoV-2) has caused incredible global disruption and challenges with a substantial impact on public health and healthcare systems (*1*). As of March 2022, the world has reported over 460 million confirmed COVID-19 cases and 6 million deaths in over 200 countries and regions (*2*). At the same time, China has had the most severe COVID-19 outbreak since the original wave from Wuhan, driven by the Omicron variant, resulting in lockdowns in Shanghai Municipality, Shenzhen City, and Jilin Province (*3–4*). For regions with high importation risk, stringent measures (e.g., reduction of international flights, post-arrival quarantine, and strict surveillance) can be applied to earn more time for preparedness and response (*5–6*). In support of this, this study estimates importation and exportation risks of various regions using nationwide mobility data in China: using Changchun City and Jilin City in Jilin Province as a case study.

METHODS

Mobility Data

This study analyzed the daily number of passengers traveling between 367 prefectures (cities) in China, including 4 municipalities, 1 special administrative region, 332 prefecture-level divisions, 6 autonomous counties, and 24 county-level cities and centrally administered municipalities. The mobility data were from a national mobile phone carrier (China Unicom), with 318 million active users in 2019, during the period from January 7 to 13, 2020 (*7–8*). When users made phone calls, sent messages, turned on/off their devices, or switched towers, the national mobile phone carrier collected their location information (*8–9*). The dataset was anonymized so that this study cannot identify or filter users of certain groups. The dataset includes approximately 100 million daily between-city trips, without overseas mobility. This research assumed that the mobility between cities for each week in this study's following simulations is the same as the study week.

Epidemic Model

Following the Covasim model structure, this study used a stochastic metapopulation model of COVID-19

transmission (Supplementary Figure S1, available in http://weekly.chinacdc.cn/) (*10*). The population is characterized as either susceptible (*S*), exposed (*E*, infected but not yet infectious), infectious (*I*), recovered (*R*), and deceased (*D*), with infectious population additionally categorized according to symptoms: pre-symptomatic (*P*), asymptomatic (*A*), mild (I_1), severe (I_2), or critical (I_3). This study set initial cases (one seed per million population) for each prefecture (city) to simulate the daily situation of disease transmission. Then, this study evaluated the mean and 95% confidence interval (CI) of the daily infected cases based on 100 simulations. Specifically, this simulation calculated the number of infected cases without severe or critical symptoms in city i at time t as follows:

$$\Lambda_i(t) = E_i(t) + P_i(t) + A_i(t) + I_{1,i}(t). \quad (1)$$

The prevalence $\xi_i(t)$ of infected cases in prefecture (city) i at time t is given by:

$$\xi_i(t) = \frac{\Lambda_i(t)}{\rho_i} \quad (2)$$

where ρ_i represents the population size of prefecture (city) i. This study then constructed an intercity mobility network to track the movement patterns of individuals between cities. Let $\omega_{o,d}(t)$ denote the number of residents from the origin prefecture (city) o that travel to the destination prefecture (city) d on day t. Given the daily prevalence $\xi_o(t)$ of prefecture (city) o, the rate at which infected residents from prefecture (city) o travel to prefecture (city) d on day t is given by $\vartheta_{o,d}(t) = \xi_o(t) \times \omega_{o,d}(t)$. The potential of importing at least one infected case from prefecture (city) o to prefecture (city) d on day t_u, is given by (*3*,*11*):

$$\psi_{o,d}(t_u) = 1 - \exp\left[-\vartheta_{o,d}(t_u)\right]. \quad (3)$$

The cumulative probability of importing at least one infection from prefecture (city) o to prefecture (city) d between t_0 and t_u is given by:

$$\kappa_{o,d}(t_u) = 1 - \exp\left[-\int_{t_0}^{t_u} \vartheta_{o,d}(u)du\right]. \quad (4)$$

For each epidemic origin, this study conducted 100 stochastic simulations across 4 months (120 days). In each simulation, the prefecture (city) d has at least 1 infected case on or by day t_u when incorporating the probability $\psi_{o,d}(t_u)$ or $\kappa_{o,d}(t_u)$, respectively. This study tracked the geographic expansion of simulated epidemics by taking each prefecture (city) as an epidemic origin (epicenter). To compare the epidemic growth across outbreak scenarios, this study measured the time until a certain percentage of prefectures (cities) with importations reaches specified thresholds, such as T=50%, and denoted this quantity as Γ_T to measure the exportation risk. To assess the epidemiological vulnerability of a specific location l, this study tracked the days until l becomes infected under various scenarios as the importation risk, χ. Matlab (version R2021b, The MathWorks, Massachusetts, US) was used for analyzing mobility data and simulating the epidemic transmission model.

RESULTS

For each possible importation location of 367 prefectures (cities), this study simulated epidemics using a stochastic epidemiological model over three transmission scenarios for the Omicron variant (different R_0): running 100 simulations for each scenario (parameters are in Supplementary Table S1, available in http://weekly. chinacdc.cn/). Under the middle transmission scenario (R_0=5.49), the cumulative infections of Changchun are estimated as 3,233 (95% CI: 1,480, 4,986) before the quarantine was imposed on March 14, 2022, which is close to the real number of cases, 3,168, reported by March 16, 2022 (*12*–*13*). This study shows the results of the middle transmission scenario in the main text and the sensitivity analysis in the supplementary.

This study estimated importation and exportation risk (Figure 1), finding that epidemics tend to spread fastest and in the shortest amount of time when imported or exported from Beijing or Shanghai. The rates at which epidemics spread from and to each prefecture (city) are highly correlated to prefectures (cities) with larger population sizes. For R_0 =5.49, 127 (35%) of 367 cities have high exportation risks and could transmit the disease to 50% of all other locations within a period from 17 to 94 days. The population sizes in the 127 prefectures (cities) with high exportation risks are around 5.69 million (95% CI: 2.08, 7.88). As a comparison, population sizes in the remaining 240 prefectures (cities) are much smaller, within 2.24 million (95% CI: 0.10, 6.09) (Supplementary Table S2, available in http://weekly. chinacdc.cn/). The importation risk, as the average time until a new infection arrives in a location in 1 of the 367 prefectures (cities), ranges from 26 to 101 days. The correlation coefficients between the population size and days of the importation and exportation risks are –0.56 and –0.77, respectively (both with P<0.001). These patterns also hold for other transmission scenarios (Supplementary Figure S2, available in http://weekly.chinacdc.cn/).

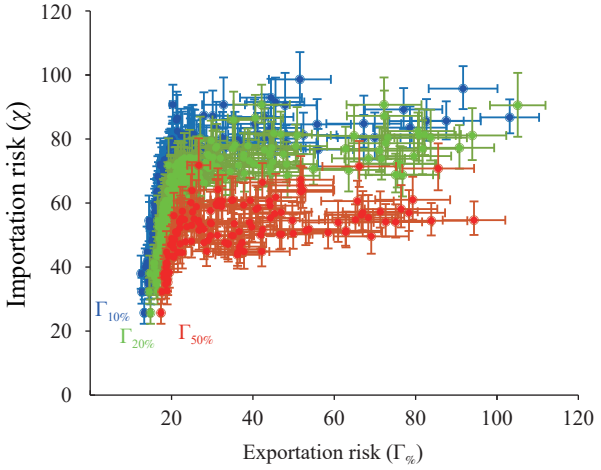

FIGURE 1. Risks of epidemic importation and exportation transmission.
Note: For each prefecture (city), the mean and 95% confidence interval (CI) of the exportation risk (x-axis) are estimated by the number of days following an importation into that prefecture (city) until 10%, 20%, and 50% of prefectures (cities) experience outbreaks ($\Gamma_{10\%}$, $\Gamma_{20\%}$, and $\Gamma_{50\%}$), averaged over 100 stochastic simulations. The mean and 95% CI of the importation risk (y-axis) are estimated by the number of days following importation in another prefecture (city) until the focal prefecture (city) receives its first infection, averaged over 100 stochastic simulations. All simulations assume an initial outbreak of R_0=5.49; analogous graphs for other R_0s are provided in Supplementary Figure S2. The importation and exportation risks are correlated with a Pearson's correlation coefficient of 0.72, and to population size of the prefecture (city) with coefficients of −0.56 and −0.77, respectively (all have *P* value <0.001).

The importation and exportation transmission risks in China are highest for outbreaks starting in Beijing and Shanghai, in terms of both geography and the underlying mobility network. In the case study of Changchun, if a city lockdown is implemented two weeks after the seeds are imported, on average 16 (95% CI: 12, 19) cities will then have imported cases from a random city. If a city lockdown is implemented one week earlier or later, on average 1 (95% CI: 1, 2) and 92 (95% CI: 86, 99) cities will have imported cases, respectively.

This study provided a data-driven modeling approach to tailoring importation and exportation risks, using Changchun and Jilin City in Jilin Province as examples (Figure 2). If transmissions start from Changchun, Harbin and Siping will have the highest probability that >1 person infected with the Omicron variant arrives from Changchun: both have a probability above 50% by March 6, 2022. In contrast, if starting from Jilin, Changchun and Harbin will have the highest probability of importation. If city lockdowns are implemented two weeks after the seeds are imported, Changchun and Jilin will introduce the disease to 18 (95% CI: 15, 21) and 8 (95% CI: 7, 9) cities in China, respectively. If the city lockdown is implemented one week earlier, they can only import to 1 (95% CI: 1, 2) and 0 (95% CI: 0, 1) cities, respectively. If it's one week later, they will import 131 (95% CI: 122, 140) and 56 (95% CI: 51, 62) cities, respectively.

DISCUSSION

Human mobility patterns shape epidemiological risk. The destiny of a newly emerging infectious disease will most likely be determined by where it was first imported. This study's analysis of prefectures (cities) in China suggests that the rate of epidemic expansion depends not only on well-understood epidemiological drivers, e.g., R_0, but also on the importation locations of the initial cases. Locations that are more vulnerable to aggressive epidemics are also the earliest to be hit by outbreaks that originate elsewhere.

Throughout the COVID-19 pandemic, as case numbers started to soar in the initial stage, countries had to make policy decisions quickly to avoid local outbreaks — even without timely and definite scientific evidence. In response to the resurgence of vaccine-evasive variants, estimation of importation risk is essential for implementing targeted risk-based travel restrictions. This study helped estimate the importation risk of prefectures (cities) from any epicenter using nationwide mobility data in China.

This study was subject to some limitations. The synthetic simulation does not explicitly include the possible delay of reports of new cases that could have happened early in the COVID-19 outbreak. In addition, this study's model does not include moderate cases directly, which are combined into severe cases. However, it does assume that asymptomatic/exposed/pre-symptomatic/mild cases can travel between prefectures (cities). Therefore, such a model design would have little impact on this study's estimates of both risk and incidence.

As Omicron outbreaks emerge within prefectures (cities) in the mainland of China in March 2022, the government will continue to face high pressure from the rapid transmissibility of the Omicron variant and coming variants in the future. The current pandemic presents a broader opportunity for us to interrogate how to control outbreaks. Like other transmissible

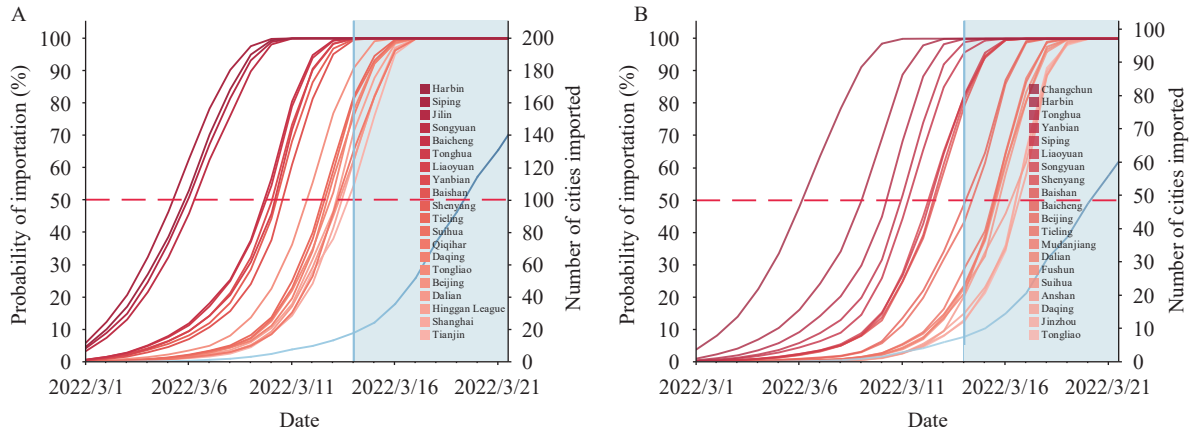

FIGURE 2. Estimated risks for importation and exportation of the SARS-CoV-2 Omicron variant over prefectures (cities) in China. (A) Changchun; (B) Jilin City.
Note: This study estimated the probability that >1 person infected with the Omicron variant arrived at the target prefecture (city) by the date indicated on the x-axis, based on China Unicom mobility data. All simulations assume an initial outbreak of R_0=5.49. This study showed the top 20 regions (with the highest probability on March 14, 2022) from cities of Changchun and Jilin City. The grey vertical line indicates March 14, 2022, the date when Jilin Province was locked down (*14*); line colours correspond to the importation risk on March 14, 2022.
Abbreviation: SARS-CoV-2=severe acute respiratory syndrome coronavirus 2.

pathogens (e.g., influenza), SARS-CoV-2 is likely to circulate in humans for many years to come (*15*). Estimating COVID-19 importation and exportation risks is necessary for preparedness and prevention and control measures of COVID-19 — especially when new variants emerge.

Acknowledgements: China Unicom, staff at the telecom carrier, Dr. Qi Tan, Dr. Bingyi Yang, Prof. Peng Jia, Prof. Xiaoke Xu, Prof. Shujuan Yang, Prof. Li Zhao, and Prof. Shiyong Liu.

Conflicts of interest: Benjamin J. Cowling consults for AstraZeneca, Fosun Pharma, GlaxoSmithKline, Moderna, Pfizer, Roche, and Sanofi Pasteur. Other authors declare no conflicts of interest.

Funding: Supported by AIR@InnoHK programme from The Innovation and Technology Commission of the Hong Kong Special Administrative Region, National Natural Science Foundation of China (72104208), JSPS KAKENHI (JP21H04595), National Nature Science Foundation of China (72025405, 91846301, 72088101, and 71790615).

doi: 10.46234/ccdcw2022.184

[#] Corresponding author: Benjamin J. Cowling, bcowling@hku.hk.

[1] WHO Collaborating Centre for Infectious Disease Epidemiology and Control, School of Public Health, Li Ka Shing Faculty of Medicine, The University of Hong Kong, Hong Kong Special Administrative Region, China; [2] Laboratory of Data Discovery for Health Limited (D^{2}4H), Hong Kong Science Park, Hong Kong Special Administrative Region, China; [3] China-Australia Joint Research Center for Infectious Diseases, School of Public Health, Xi'an Jiaotong University Health Science Center, Xi'an City, Shaanxi Province, China; [4] Department of Genetics, University of Cambridge, Cambridge CB2 3EH, UK; [5] College of Systems Engineering, National University of Defense Technology, Changsha City, Hunan Province, China; [6] Department of Computer Science, Aalto University, Espoo, Finland; [7] Center for Computational Social Science, Kobe University, Kobe, Japan.
[&] Joint first authors.

Submitted: April 29, 2022; Accepted: August 21, 2022

REFERENCES

1. Chakraborty I, Maity P. COVID-19 outbreak: migration, effects on society, global environment and prevention. Sci Total Environ 2020;728:138882. http://dx.doi.org/10.1016/j.scitotenv.2020.138882.
2. WHO. Novel Coronavirus (2019-nCoV) situation reports [Internet]. 2022. https://www.who.int/emergencies/diseases/novel-coronavirus-2019/situation-reports. [2022-5-30].
3. Du ZW, Wang L, Cauchemez S, Xu XK, Wang XW, Cowling BJ, et al. Risk for transportation of coronavirus disease from Wuhan to other cities in China. Emerg Infect Dis 2020;26(5):1049 – 52. http://dx.doi.org/10.3201/eid2605.200146.
4. Ruktanonchai NW, Floyd JR, Lai S, Ruktanonchai CW, Sadilek A, Rente-Lourenco P, et al. Assessing the impact of coordinated COVID-19 exit strategies across Europe. Science 2020;369(6510):1465 – 70. http://dx.doi.org/10.1126/science.abc5096.
5. Nakamura H, Managi S. Airport risk of importation and exportation of the COVID-19 pandemic. Transp Policy 2020;96:40 – 7. http://dx.doi.org/10.1016/j.tranpol.2020.06.018.
6. Lee K, Worsnop CZ, Grépin KA, Kamradt-Scott A. Global coordination on cross-border travel and trade measures crucial to COVID-19 response. Lancet 2020;395(10237):1593 – 5. http://dx.doi.org/10.1016/S0140-6736(20)31032-1.
7. Slotta D. Number of China Unicom mobile subscriptions from 2011 to 2021 [Internet]. 2022. https://www.statista.com/statistics/233968/number-of-china-unicom-mobile-subscriptions. [2022-3-17].
8. Tan SY, Lai SJ, Fang F, Cao ZQ, Sai B, Song B, et al. Mobility in China, 2020: a tale of four phases. Natl Sci Rev 2021;8(11):nwab148. http://dx.doi.org/10.1093/nsr/nwab148.
9. Gao C, Liu JM. Modeling and restraining mobile virus propagation.

IEEE Trans Mob Comput 2013;12(3):529 – 41. http://dx.doi.org/10.1109/TMC.2012.29.
10. Kerr CC, Stuart RM, Mistry D, Abeysuriya RG, Rosenfeld K, Hart GR, et al. Covasim: an agent-based model of COVID-19 dynamics and interventions. PLoS Comput Biol 2021;17(7):e1009149. http://dx.doi.org/10.1371/journal.pcbi.1009149.
11. Wang L, Wu JT. Characterizing the dynamics underlying global spread of epidemics. Nat Commun 2018;9(1):218. http://dx.doi.org/10.1038/s41467-017-02344-z.
12. Ruan F, Zhang XB, Xiao SJ, Ni XH, Yin XL, Ye ZW, et al. An outbreak of the SARS-CoV-2 omicron variant BA.1 — Zhuhai City, Guangdong Province, China, January 13, 2022. China CDC Wkly 2022;4(30):669-71. http://dx.doi.org/10.46234/ccdcw2022.032.
13. Changchun Municipal Health Commission. Changchun Municipal Health Commission's briefing on the new crown pneumonia epidemic situation [Internet]. 2022. http://wjw.changchun.gov.cn/xwzx/tzgg/202203/t20220318_2994637.html. [2022-3-18]. (In Chinese).
14. Leading Group for Prevention and Control of COVID-19 in Jilin Province. Jilin Province: from today, the movement of people in this province across provinces, cities and states is prohibited [Internet]. 2022. http://www.news.cn/local/2022-03/14/c_1128469069.htm. [2022-3-18]. (In Chinese).
15. Cobey S. Modeling infectious disease dynamics. Science 2020;368(6492):713 – 4. http://dx.doi.org/10.1126/science.abb5659.

SUPPLEMENTARY MATERIAL

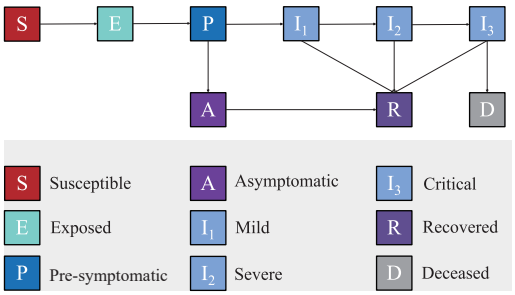

SUPPLEMENTARY FIGURE S1. Schematic of the model structure, following the Covasim model structure (*1*).
- An individual must pass through a mild stage before reaching a severe or critical stage.
- An individual must pass through a severe stage before reaching a critical stage.
- Only individuals in a critical stage may die.
- All individuals have equal transmission rates and equal susceptibility to infection.
- The transmission rate of severe or critical infections will not be involved in the calculation of mobility prevalence, because we assume that infected patients will be hospitalized when symptoms become severe or critical.

SUPPLEMENTARY TABLE S1. Epidemiological parameters.

Parameters	Values (mean, std)	Data source
R_0: basic reproduction number	2.43 (5.49, 8)	Given that the effective reproduction number (R_e) of the Omicron variant of SARS-CoV-2 is estimated at 2.43 (95% CI: 1.05, 5.49) in China (*2*) and around 8 in South Africa (*3*), we study the basic reproduction number (R_0) in the range from 2.43, 5.49 to 8. (*2–3*)
β: transmission rate per contact for a symptomatic case (mild, severe, critical)	Calibrated to R_0	Assumed
ω_p: relative infectiousness of pre-symptomatic cases as compared to symptomatic cases	1.57	(*4–5*)
ω_a: relative infectiousness of asymptomatic cases as compared to symptomatic cases	0.5	(*6*)
ρ_i: initial cases	One seed per million population	Assumed
T_{inf}: latent period	Lognormal (4.5, 1.5)	(*7–8*)
T_{pre}: duration of pre-symptomatic infectiousness (length of duration after viral shedding has begun before an individual has symptoms)	2	(*9*)
T_m: duration of mild symptomatic infectiousness	Lognormal (6.6, 4.9)	(*10–11*)
T_s: duration of severe symptomatic infectiousness	Lognormal (1.5, 2.0)	(*11–12*)
T_c: duration of critical symptomatic infectiousness	Lognormal (10.7, 4.8)	(*13*)
T_a: duration of asymptomatic infectiousness	Lognormal (8.0, 2.0)	(*14*)
F_a: fraction of asymptomatic infectiousness	27%	(*15*)
F_s: fraction of (symptomatic) infections that are severe	0.8%	Assumed
F_c: fraction of (symptomatic) infections that are critical	0.1%	Assumed
CFR: Case fatality rate (fraction of infections that eventually result in decease)	0.1%	Assumed
α_0: transition rate out of exposed state	$1 / T_{inf}$	
α_1: transition rate out of pre-symptomatic state to symptomatic state	$1 - F_a$	
α_m: transition rate out of mild infectiousness state	$(1 / T_m) - \gamma_m$	
α_s: transition rate out of severe infectiousness state	$(1 / T_s) * (F_c/F_s+F_c)$	
α_c: transition rate out of critical infectiousness state	$(1 / T_c) * (\text{CFR} / F_c)$	(16)
γ_m: recovery rate of mild symptomatic individuals	$(1 / T_m) * (1 - F_a)$	
γ_s: recovery rate of severe symptomatic individuals	$(1 / T_s) - \alpha_s$	
γ_c: recovery rate of critical symptomatic individuals	$(1 / T_c) - \alpha_c$	
γ_a: recovery rate of asymptomatic individuals	$1 / T_a$	

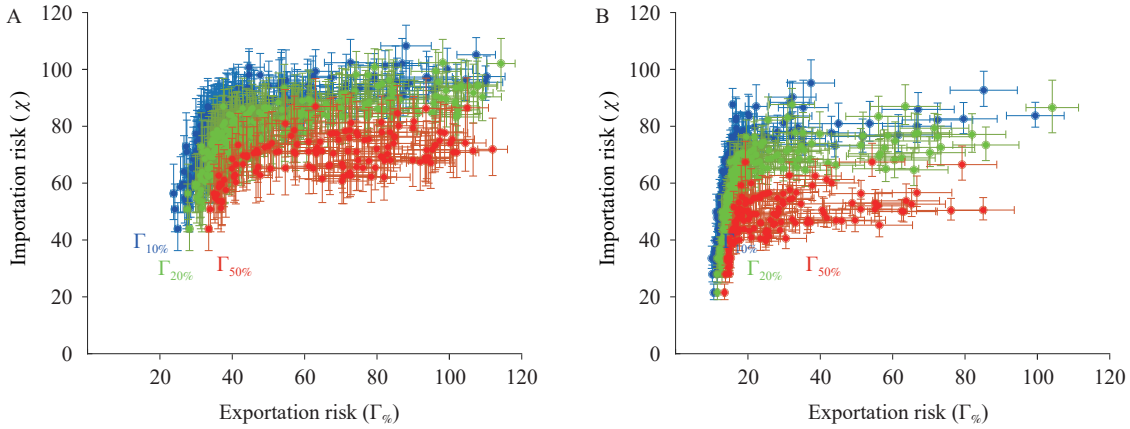

SUPPLEMENTARY FIGURE S2. Risks of epidemic importation and exportation transmission with different R_0, (A) R_0=2.43 and (B) R_0=8.

Note: For each prefecture (city), the mean and 95% CI of the exportation risk (x-axis) are estimated by the number of days following an importation into that prefecture (city) until 10%, 20%, and 50% of prefectures (cities) experience outbreaks ($\Gamma_{10\%}$, $\Gamma_{20\%}$, and $\Gamma_{50\%}$), averaged over 100 stochastic simulations. The mean and 95% CI of the importation risk (y-axis) are estimated by the number of days following importation in another prefecture (city) until the focal prefecture (city) receives its first infection, averaged over 100 stochastic simulations of (A) R_0=2.43 and (B) R_0=8. The importation and exportation risks are correlated with a Pearson's correlation coefficient of (A) 0.72 and (B) 0.72, and to population size of the prefecture (city) with coefficients of (A) –0.55 and –0.76; (B) –0.56 and –0.77, respectively (all have *P*-value <0.001).

SUPPLEMENTARY TABLE S2. List of 51 study regions including 28 provincial capitals, 4 municipalities, 1 special administrative region of China, and the prefectures (cities).

Prefecture (city)	Population	$\Gamma_{10\%}$		$\Gamma_{20\%}$		$\Gamma_{50\%}$	
		Exportation risk (mean)	Importation risk (mean)	Exportation risk (mean)	Importation risk (mean)	Exportation risk (mean)	Importation risk (mean)
Chongqing	30,752,000	14.74	36.38	16.58	36.38	19.01	36.38
Shanghai	24,183,000	12.72	32.26	14.53	32.26	17.63	32.26
Beijing	21,707,000	13.28	25.70	14.82	25.70	17.40	25.70
Chengdu	16,044,700	14.34	34.64	16.30	34.64	18.53	34.64
Tianjin	15,569,000	14.96	38.32	16.50	38.32	19.45	38.32
Guangzhou	14,498,400	12.53	37.96	14.64	37.96	18.11	37.96
Harbin	10,929,000	16.38	57.43	17.63	57.43	22.65	57.43
Wuhan	10,892,900	14.19	36.84	15.83	36.84	18.17	36.84
Shijiazhuang	10,879,900	16.66	47.24	17.96	47.24	22.10	47.24
Zhengzhou	9,880,000	14.85	32.61	16.56	32.61	18.91	32.61
Hangzhou	9,468,000	14.00	41.27	15.63	41.27	18.82	41.27
Xi'an	8,989,000	14.38	35.25	16.21	35.25	19.05	35.25
Nanjing	8,335,000	14.13	41.19	15.86	41.19	18.88	41.19
Shenyang	8,294,000	15.38	50.44	17.36	50.44	21.37	50.44
Hefei	7,965,300	14.90	43.38	17.01	43.38	20.28	43.38
Changsha	7,918,100	14.59	38.07	16.17	38.07	18.50	38.07
Changchun	7,674,439	16.64	60.64	18.85	60.64	31.49	60.64
Hong Kong	7,413,100	51.55	98.63	–	98.63	–	98.63
Jinan	7,321,200	15.68	43.13	17.28	43.13	20.57	43.13
Nanning	7,153,300	15.94	50.91	17.54	50.91	21.34	50.91
Dalian	6,988,000	16.38	58.84	18.18	58.84	26.09	58.84
Kunming	6783,,000	14.73	44.61	16.23	44.61	18.77	44.61

TABLE S2. (Continued)

Prefecture (city)	Population	$\Gamma_{10\%}$		$\Gamma_{20\%}$		$\Gamma_{50\%}$	
		Exportation risk (mean)	Importation risk (mean)	Exportation risk (mean)	Importation risk (mean)	Exportation risk (mean)	Importation risk (mean)
Nanchang	5,463,538	15.20	43.39	16.38	43.39	19.25	43.39
Suihua	5,418,153	20.76	69.19	37.94	69.19	–	69.19
Qiqihar	5,367,003	21.61	70.76	54.90	70.76	–	70.76
Guiyang	4,802,000	15.85	45.97	17.22	45.97	20.44	45.97
Jilin	4,413,157	18.98	68.08	26.78	68.08	–	68.08
Taiyuan	4,379,700	16.65	53.93	18.17	53.93	22.03	53.93
Fuzhou	4,031,037	16.69	52.55	17.95	52.55	39.71	52.55
Lanzhou	3,729,600	16.78	55.24	18.44	55.24	22.48	55.24
Anshan	3,598,000	19.18	70.13	26.05	70.13	–	70.13
Urumqi	3,500,000	17.24	71.81	19.27	71.81	26.68	71.81
Siping	3,385,156	18.73	68.53	48.51	68.53	–	68.53
Tongliao	3,128,700	19.58	70.33	63.55	70.33	–	70.33
Hohhot	3,114,800	17.74	67.28	20.40	67.28	51.74	67.28
Jinzhou	3,050,000	18.47	67.81	25.36	67.81	–	67.81
Daqing	2,904,532	21.26	75.69	44.21	75.69	–	75.69
Songyuan	2,880,086	20.17	68.84	75.10	68.84	–	68.84
Mudanjiang	2,798,723	25.45	70.46	–	70.46	–	70.46
Tieling	2,638,000	20.06	69.67	44.44	69.67	–	69.67
Xining	2,355,000	18.72	67.88	22.32	67.88	–	67.88
Tonghua	2,324,439	23.97	68.81	76.77	68.81	–	68.81
Haikou	2,272,100	16.03	56.04	17.71	56.04	20.58	56.04
Yanbian Korean Autonomous Prefecture	2,270,816	20.65	72.24	75.50	72.24	–	72.24
Yinchuan	2,225,391	18.27	71.43	21.71	71.43	66.14	71.43
Fushun	2,065,000	20.97	71.32	31.23	71.32	–	71.32
Baicheng	2,032,356	22.18	74.67	79.59	74.67	–	74.67
Baishan	1,296,127	24.82	72.66	–	72.66	–	72.66
Hinggan League	1,604,200	23.45	76.48	–	76.48	–	76.48
Liaoyuan	1,176,239	25.02	71.88	–	71.88	–	71.88
Lhasa	559,423	21.44	86.53	40.61	86.53	–	86.53

Note: For each prefecture (city), the mean estimates of the exportation risk and the importation risk are calculated until 10%, 20%, and 50% of prefectures (cities) experience outbreaks ($\Gamma_{10\%}$, $\Gamma_{20\%}$, and $\Gamma_{50\%}$), averaged over 100 stochastic simulations. All simulations assume an initial outbreak of R_0= 5.49.
"–" denotes regions without any importations or exportations in the studied period.

REFERENCES

1. Kerr CC, Stuart RM, Mistry D, Abeysuriya RG, Rosenfeld K, Hart GR, et al. Covasim: An agent-based model of COVID-19 dynamics and interventions. PLoS Comput Biol 2021;17(7):e1009149. http://dx.doi.org/10.1371/journal.pcbi.1009149.
2. Ruan F, Zhang X, Xiao S, Ni X, Yin X, Ye Z, et al. An Outbreak of the COVID-19 Omicron Variant — Zhuhai City, Guangdong Province, China, January 13, 2022. China CDC Wkly 2022;4(30);669–71. https://doi.org/10.46234/ccdcw2022.032.
3. Nishiura H, Ito K, Anzai A, Kobayashi T, Piantham C, Rodríguez-Morales AJ. Relative reproduction number of SARS-CoV2 Omicron (B.1.1.529) compared with Delta Variant in South Africa. J Clin Med Res 2021;11(1). Available from: http://dx.doi.org/10.3390/jcm11010030.
4. Aleta A, Martín-Corral D, Pastore Y Piontti A, Ajelli M, Litvinova M, Chinazzi M, et al. Modelling the impact of testing, contact tracing and household quarantine on second waves of COVID-19. Nat Hum Behav 2020;4(9):964–71. https://doi.org/10.1038/s41562-020-0931-9.
5. He X, Lau EHY, Wu P, Deng X, Wang J, Hao X, et al. Temporal dynamics in viral shedding and transmissibility of COVID-19. Nat Med 2020;26(5):672 – 5. http://dx.doi.org/10.1038/s41591-020-0869-5.
6. Evoy DM, Mc Evoy D, McAloon CG, Collins ÁB, Hunt K, Butler F, et al. The relative infectiousness of asymptomatic SARS-CoV-2 infected persons

compared with symptomatic individuals: A rapid scoping review. https://doi:10.1136/bmjopen-2020-042354.
7. Lauer SA, Grantz KH, Bi Q, Jones FK, Zheng Q, Meredith HR, et al. The Incubation Period of Coronavirus Disease 2019 (COVID-19) From Publicly Reported Confirmed Cases: Estimation and Application. Ann Intern Med 2020;172(9):577–82. https://doi.org/10.7326/M20-0504.
8. Pung R, Chiew CJ, Young BE, Chin S, Chen MI-C, Clapham HE, et al. Investigation of three clusters of COVID-19 in Singapore: implications for surveillance and response measures. Lancet 2020;395(10229):1039–46. https://doi.org/10.1016/S0140-6736(20)30528-6.
9. Du Z, Xu X, Wu Y, Wang L, Cowling BJ. Serial interval of COVID-19 among publicly reported confirmed cases. Emerg Infect Dis 2020;26(6):1341. http://dx.doi.org/10.3201/eid2606.200357.
10. Linton NM, Kobayashi T, Yang Y, Hayashi K, Akhmetzhanov AR, Jung SM, et al. Incubation Period and Other Epidemiological Characteristics of 2019 Novel Coronavirus Infections with Right Truncation: A Statistical Analysis of Publicly Available Case Data. J Clin Med Res 2020;9(2):538. http://dx.doi.org/10.3390/jcm9020538.
11. Wang D, Hu B, Hu C, Zhu F, Liu X, Zhang J, et al. Clinical Characteristics of 138 Hospitalized Patients With 2019 Novel Coronavirus-Infected Pneumonia in Wuhan, China. JAMA 2020;323(11):1061–9. https://doi.org/10.1001/jama.2020.1585.
12. Chen J, Qi T, Liu L, Ling Y, Qian Z, Li T, et al. Clinical progression of patients with COVID-19 in Shanghai, China. J Infect 2020;80(5):e1 – 6. http://dx.doi.org/10.1016/j.jinf.2020.03.004.
13. Verity R, Okell LC, Dorigatti I, Winskill P, Whittaker C, Imai N, et al. Estimates of the severity of coronavirus disease 2019: a model-based analysis. Lancet Infect Dis 2020;20(6):669 – 77. http://dx.doi.org/10.1016/S1473-3099(20)30243-7.
14. Wölfel R, Corman VM, Guggemos W, Seilmaier M, Zange S, Müller MA, et al. Virological assessment of hospitalized patients with COVID-2019. Nature 2020;581(7809):465 – 9. http://dx.doi.org/10.1038/s41586-020-2196-x.
15. Kappler M. People with Omicron much more likely to be asymptomatic, research suggests [Internet]. Available from: https://www.healthing.ca/diseases-and-conditions/coronavirus/omicron-asymptomatic-rate. [2022-03-19].
16. Modeling COVID-19 spread vs healthcare capacity [Internet]. https://alhill.shinyapps.io/COVID19seir. [2022-5-19].

Methods and Applications

Detection of SARS-CoV-2 Antibodies in Oral Fluid Using a Magnetic Particle-Based Chemiluminescence Immunoassay — Beijing Municipality, China, 2021

Naiying Mao[1,&]; Mei Dong[2,&]; Zhen Zhu[1]; Qi Huang[2]; Xiali Yu[2]; Hui Xie[2]; Jianping Dong[3]; Jingyi Sun[3]; Fang Huang[2,#]; Wenbo Xu[1,#]

ABSTRACT

Introduction: Oral fluids (OFs) have been broadly used as non-invasive samples for evaluating protective IgG antibodies from natural infection or vaccination, especially in pediatric populations.

Methods: Paired OF and serum were collected from both individuals who received a booster dose of the inactive coronavirus disease 2019 (COVID-19) vaccine as well as those who did not have a history of COVID-19 vaccination and infection (as the control group). The total human IgG antibody (HIgG) content was evaluated as a marker of OF sampling quality. An in-house adapted magnetic particle-based chemiluminescence immunoassay was used for severe acute respiratory syndrome coronavirus 2 (SARS-CoV-2) IgG antibody detection in the OF. The SARS-CoV-2 IgG antibody in the serum samples was detected using a commercial immunoassay.

Results: In total, 579 paired OF and serum samples were collected. An additional 172 OF samples were collected from preschool children. The results indicated that the HIgG concentration in qualified OF samples should be higher than 0.3 μg/mL. Compared to the serum assay, the in-house OF immunoassay for detecting IgG antibodies against SARS-CoV-2 had 95.06% accuracy, 95.03% sensitivity, and 100% specificity.

Conclusions: Overall, the in-house immunoassay for detecting SARS-CoV-2 IgG antibodies in OF showed high potential for application towards serological surveillance and immunization effect assessment after large-scale, inactive COVID-19 vaccination in China.

INTRODUCTION

Since the beginning of the coronavirus disease 2019 (COVID-19) pandemic, caused by severe acute respiratory syndrome coronavirus 2 (SARS-CoV-2), more than 440 million people have been infected and 6 million have died worldwide as of March 2022: posing a serious public health challenge (*1*). Vaccination provides robust protection for preventing and controlling the spread of COVID-19 (*2*). However, although the largest scale COVID-19 vaccination yet has been launched in China, outbreaks of COVID-19 are still occurring across the country (*3*–*5*). Sero-epidemiological investigations are key to evaluating whether a population has reached an effective immunization barrier and to finding any immunization gaps (*6*). A crucial hindrance to such investigations, particularly in young children, is the feasibility of collecting large-scale representative blood samples. Oral fluid (OF) has been successfully used for decades to evaluate the antibody levels of childhood immunization programs for measles and rubella (*7*). OF is a mixed exudate derived from several anatomical sources, including the saliva and gingival crevicular fluid, which contains the same IgG and IgM antibodies as those in the serum. Detection of SARS-CoV-2-induced antibodies in OF can thus provide a non-invasive method for assessing host responses to infection or vaccination.

In this study, an adapted magnetic particle-based chemiluminescence immunoassay (CLIA) was developed to detect IgG antibodies against SARS-CoV-2 in OF. Recipients of inactivated vaccines against COVID-19 were recruited and paired serum and OF samples were collected for comparison. Further, the sensitivity and specificity of this non-invasive immunoassay (OF assay) for SARS-CoV-2 IgG antibody detection were evaluated.

METHODS

Paired serum and OF samples were collected from individuals who had received a booster dose (third

dose) of inactive COVID-19 vaccine (vaccine group) as well as those who were a part of the population that was unvaccinated or uninfected with COVID-19 (control group). In the vaccine group, participants were voluntarily recruited from the Beijing Center for Disease Control and Prevention and from Beijing Haidian Hospital in November 2021. In the control group, due to the high coverage rate of COVID-19 vaccine in Beijing in 2021, individuals who had collected paired serum and OF samples in 2018 before the COVID-19 pandemic were included from Beijing Haidian Hospital. Additionally, OF samples from healthy preschool children who were not vaccinated because of the COVID-19 immunization age restriction were also collected to assess the quality of pediatric OF sampling. All participants and guardians, on behalf of the pre-school children, provided written informed consent prior to enrollment in the study.

The self-collection device (Oracol, S10, Malvern Medical Developments, UK) was used to collect OF samples (according to the manufacturer's instructions). As a brief overview, the sponge swab was brushed at the junction between the teeth and gums of participants repeatedly for at least 90 seconds until completely soaked, and then placed back into the tube and capped. OF was extracted using 0.6 mL elution buffer (phosphate-buffered saline containing 10% fetal calf serum, 500 μg/mL gentamicin, and 1 mL penicillin-streptomycin solution). The tube was centrifuged at 250 ×*g* for 1 minute to remove cellular debris; then, the sponge swab was removed and discarded. Next, the supernatant OF was collected for further analysis. Blood samples were collected in blood collection tubes (Becton, Dickinson and Company) and stored at room temperature until coagulated before being transported to the laboratory. The blood samples were then centrifuged at 1,500 ×*g* for 10 minutes to separate the serum.

For detecting SARS-CoV-2 IgG antibodies in OF, an adapted in-house SARS-CoV-2 IgG magnetic particle-based CLIA for OF was developed (*8*). Simply, 75 μL of OF samples and 50 μL of recombinant SARS-CoV-2 antigens, labeled with fluorescein isothiocyanate (FITC), were added into a reaction tube to form the antigen-antibody complex. Meanwhile, 35 μL of magnetic particles conjugated with anti-FITC antibodies were added and incubated at 37 °C for 20 minutes to form IgG antibody-antigen-magnetic particle complexes. After washing away the unbound components, 75 μL of alkaline phosphatase-labeled mouse anti-human IgG monoclonal antibody was added. After incubation, the complex was washed again; finally, 100 μL of substrate solution was added, and the chemiluminescence value of each OF sample was measured.

For detection of SARS-CoV-2 IgG antibody in the serum, a commercial SARS-CoV-2 IgG magnetic particle-based CLIA (Bioscience, Tianjin, China; Lot number: G202108003) was used according to the manufacturer's protocol. The SARS-CoV-2 IgG antibody levels are presented as a ratio (S/CO, chemiluminescence value of sample/cutoff value). Samples with ratios exceeding or equal to 1 were considered positive and those with ratios of less than 1 were considered negative.

To ensure the quality of OF sampling, the total human IgG antibody (HIgG) content in the OF was selected as the biological index for sampling quality. The content of HIgG in each OF sample was measured using an HIgG antibody detection kit (Bioscience, Tianjin, China; Lot number: G202108003). A reference value range (one-sided) of 95% of HIgG was evaluated to establish the quality standard of OF sampling.

The sensitivity and specificity of the OF immunoassay for SARS-CoV-2 IgG detection were calculated and compared to those of a commercial magnetic particle-based CLIA. The best cutoff value for the in-house OF immunoassay was assessed using receiver operating characteristic curve (ROC) analysis. The Pearson chi-square test was used to test the differences among sampling methods. Statistical analysis and ROC analysis were performed using SPSS software (version 19, IBM, NY, USA). A value of *P* less than 0.05 was considered statistically significant.

RESULTS

During the study period, a total of 579 paired serum and OF samples were collected, with 364 and 215 from the vaccine and control group, respectively. The median age of the participants in the vaccine group was 45 years (interquartile range [IQR], 35–53 years). In the control group, the median age was 34 years (IQR, 29–39 years). Further, 172 OF samples were collected from preschool children with a median age of 4 years (IQR, 3–5 years).

To evaluate the quality of OF sampling, the total HIgG concentrations in 751 OF samples (579 adults and 172 children) were determined. Overall, the mean concentration of HIgG in OF samples was 1.85± 0.83 μg/mL. The mean concentration of HIgG in OF

samples from children was 2.02±1.02 μg/mL, which was significantly higher than that of the adults at 1.85±0.77 μg/mL (t=2.223, P<0.05). Further, the mean HIgG concentration in the OF samples from the vaccine group was 2.01±0.72 μg/mL, which was significantly higher than that of the control group at 1.59±0.77 μg/mL (t=6.616, P<0.001) (Figure 1). However, there was no significant correlation between the HIgG concentration in the OF and the titer of IgG antibody against SARS-CoV-2 in the serum (R^2=0.062). The threshold for HIgG concentration in qualified OF samples could be set to 0.3 μg/mL, as more than 95% of OF samples contained higher concentrations of HIgG. Based on this cutoff, 8 and 12 OF samples from the vaccine and control groups, respectively, were excluded from the study.

The SARS-CoV-2 IgG antibody was detected in 397 paired OF and serum samples (194 from the vaccine group and 203 from the control group) using both the adapted in-house immunoassay and commercial magnetic particle-based CLIA. Compared to the titer of SARS-CoV-2 IgG in serum, a ROC curve was plotted for detecting SARS-CoV-2 IgG antibody in OF samples. The area under the ROC curve for SARS-CoV-2 IgG antibody in OF samples was 0.988, and the chemiluminescence cutoff value was set as 105,566.5 (Figure 2).

Based on the cutoff value of SARS-CoV-2 IgG antibodies in the OF, among 162 paired OF and serum samples in the vaccine group, 161 (99.38%) serum samples and 153 OF samples (94.44%) tested positive for SARS-CoV-2 IgG (Table 1). Compared with the serum test, the in-house OF assay had 95.06% accuracy, 95.03% sensitivity, and 100% specificity. Of the eight false-negative OF samples, the range of S/CO values in the OF samples was 0.187–0.881, whereas that in the matched serum samples was 1.574–10.776. The concentration of SARS-CoV-2 IgG in OF was significantly correlated with that of the serum (R^2=0.62, P<0.001) (Figure 3).

DISCUSSION

To date, several assays for the non-invasive detection of SARS-CoV-2 antibodies in OF have been established using different methods, such as enzyme-linked immunosorbent assays (ELISA) or lateral flow immune assays (LFIA) (*9*). However, the sensitivity of these commercial assays ranges from 53%–80%, which may not meet the requirements of the antibody prevalence survey (*9*–*10*). In this study, we evaluated a magnetic particle-based CLIA with high sensitivity to detect SARS-CoV-2 IgG antibodies in OF; this assay combined several advantages, including high sensitivity, high-throughput, and non-invasiveness. The in-house OF immunoassay showed that the SARS-CoV-2 specific IgG antibody levels in OF were similar to those observed in the serum, with 95.06% concordance. This assay achieved 95.03% sensitivity,

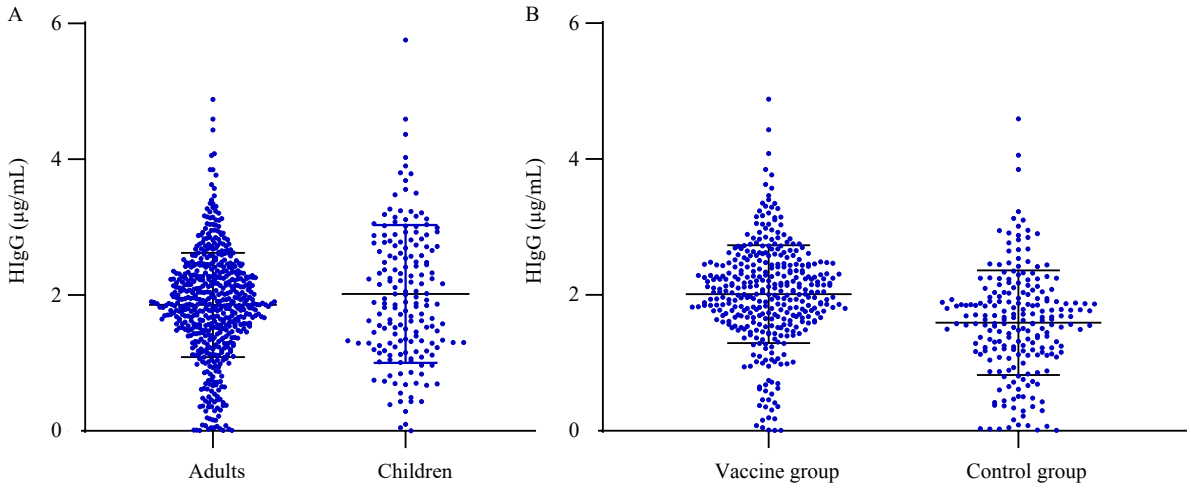

FIGURE 1. The distribution of HIgG titers in OF samples based on age and immune state. (A) The different levels of HIgG antibodies between adults group (over 18 years old) and children group (younger than 14 years); (B) The different levels of HIgG antibodies between vaccine group (received booster dose of COVID-19 vaccine) and control group (without COVID-19 infection or vaccination history).
Abbreviation: HIgG=human immunoglobulin G; OF=oral fluid; SARS-CoV-2=severe acute respiratory syndrome coronavirus 2; COVID-19=coronavirus disease 2019.

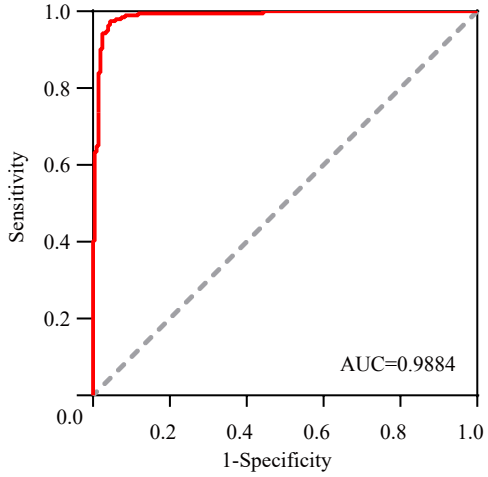

FIGURE 2. The ROC curve for SARS-CoV-2 IgG antibody detection in OF samples.
Note: The true positive rate (sensitivity) of SARS-CoV-2 IgG antibodies in OF is plotted in function of the false positive (1-specificity) for different cut-off points.
Abbreviation: ROC=receiver operating characteristic; OF=oral fluid; AUC=area under curve; SARS-CoV-2=severe acute respiratory syndrome coronavirus 2.

TABLE 1. Comparison of SARS-CoV-2 IgG antibody levels between the OF and serum samples in the vaccine group.

Detection of SARS-CoV-2 IgG		SARS-CoV-2 IgG in serum		Total
		Positive	Negative	
SARS-CoV-2 IgG in OF	Positive	153	0	153
	Negative	8	1	9
	Total	161	1	162

Abbreviation: SARS-CoV-2=severe acute respiratory syndrome coronavirus 2; OF=oral fluid.

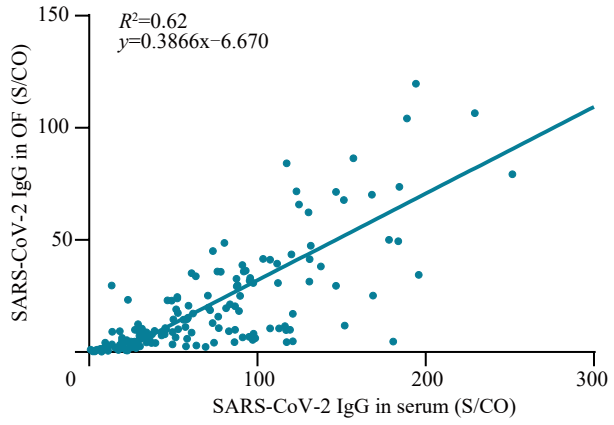

FIGURE 3. The correlation analysis of SARS-CoV-2 IgG between OF and serum samples.
Note: Scatter plots of S/CO value of SARS-CoV-2 IgG concentration in OF (y-axis) and S/CO value of SARS-CoV-2 IgG concentration in serum (x-axis).
Abbreviation: SARS-CoV-2=severe acute respiratory syndrome coronavirus 2; S/CO=chemiluminescence value of sample/cutoff value; OF=oral fluid.

which was higher than that of the above mentioned, commercial, non-invasive assays for SARS-CoV-2 specific antibody detection.

The OF comprises saliva and gingival crevicular fluid, which is rich in human IgG antibodies, but only represents a 1/1,000 dilution of that of the serum (*11*). Therefore, the quality of OF collection is critical for detecting SARS-CoV-2 IgG antibodies using the in-house OF assay. In this study, each participant was instructed by healthcare workers to brush the gumline at least for 90 seconds to stimulate the transudation of fluid. Further, the total HIgG content of each OF sample was measured to monitor the process of OF sampling. The threshold of HIgG for qualified OF samples was set as 0.3 μg/mL. Previous studies reported that the HIgG concentration in OF from children was lower than that in adults (*9*). However, our results indicate that OF samples from children have higher HIgG levels than those from adults. Further studies need to be conducted to clarify this phenomenon. In addition, vaccinated adults were found to have higher concentrations of total HIgG in OF than those in unvaccinated adults, possibly because of their active immune status at the time of OF sample collection.

However, this study has several limitations. First, as the quality of self-collected OF is highly dependent on proper operation and ease of using the collection device, the difference in total HIgG contents between samples from children and adults might be attributed to sampling bias; at the same time, all OF samples were collected only from adults over 18 years old and children under 14 years old, which also may lead to sampling bias. Second, the paired OF and serum samples in this study were only collected from the adult population and were not representative of the SARS-CoV-2 antibody in the OF from children and elderly individuals. Finally, the SARS-CoV-2 IgG antibody levels in OF from patients with COVID-19 have not been assessed in this study.

In summary, our results demonstrate the high potential of OF as a replacement for serum for serological surveillance and immunization effect assessment in the context of large-scale immunization programs for the inactivated COVID-19 vaccine in China. However, further studies are needed to improve the performance of the in-house OF assay, including enhancement of thermal stability, quantification, and standardization of the SARS-CoV-2 IgG titers in OF samples.

Funding: Supported by the Capital's Funds for

Health Improvement and Research (2021-1G-3011).

doi: 10.46234/ccdcw2022.185

[#] Corresponding authors: Fang Huang, hhffxdd@126.com; Wenbo Xu, xuwb@ivdc.chinacdc.cn.

[1] NHC Key Laboratory of Medical Virology and Viral Diseases, WHO WPRO Regional Reference Laboratory of Measles and Rubella, Measles Laboratory in National Institute for Viral Disease Control and Prevention, Chinese Center for Disease Control and Prevention, Beijing, China; [2] Institute for Immunization and Prevention, Beijing Center for Disease Control and Prevention, Beijing Academy for Preventive Medicine, Beijing Institute of Tuberculosis Control Research and Prevention, Beijing, China; [3] Department of Infectious Diseases, Beijing Haidian Hospital, Beijing Haidian Section of Peking University Third Hospital, Beijing, China.
[&] Joint first authors.

Submitted: September 13, 2022; Accepted: October 04, 2022

REFERENCES

1. World Health Organization. Coronavirus disease (COVID-19) situation reports. 2022. https://www.who.int/emergencies/diseases/novel-coronavirus-2019. [2022-3-12].
2. Feng S, Phillips DJ, White T, Sayal H, Aley PK, Bibi S, et al. Correlates of protection against symptomatic and asymptomatic SARS-CoV-2 infection. Nat Med 2021;27(11):2032 – 40. http://dx.doi.org/10.1038/s41591-021-01540-1.
3. Zhang M, Xiao JP, Deng AP, Zhang YT, Zhuang YL, Hu T, et al. Transmission dynamics of an outbreak of the COVID-19 delta variant B.1.617.2 - Guangdong province, China, May-June 2021. China CDC Wkly, 2021;3(27):584-6. http://dx.doi.org/10.46234/ccdcw2021.148.
4. Liu SW, Yuan SH, Sun YQ, Zhang BG, Wang HZ, Lu JX, et al. A COVID-19 outbreak - Nangong city, Hebei province, China, January 2021. China CDC Wkly 2021;3(19):401 – 4. http://dx.doi.org/10.46234/ccdcw2021.077.
5. Hou L, Zhou H, Meng NX, Yu X, Wang X, Wang T, et al. A COVID-19 outbreak emerging in a food processing company — Harbin city, Heilongjiang province, China, January–February 2021. China CDC Wkly 2021;3(32):681 – 7. http://dx.doi.org/10.46234/ccdcw2021.153.
6. Li ZJ, Guan XH, Mao NY, Luo HM, Qin Y, He N, et al. Antibody seroprevalence in the epicenter Wuhan, Hubei, and six selected provinces after containment of the first epidemic wave of COVID-19 in China. Lancet Reg Health West Pac 2021;8:100094. http://dx.doi.org/10.1016/j.lanwpc.2021.100094.
7. Perry KR, Brown DWG, Parry JV, Panday S, Pipkin C, Richards A. Detection of measles, mumps, and rubella antibodies in saliva using antibody capture radioimmunoassay. J Med Virol 1993;40(3):235 – 40. http://dx.doi.org/10.1002/jmv.1890400312.
8. Huang Q, Liu FY, Mao NY, Sun JY, Dong M, Xie H, et al. Application of oral fluid in SARS-CoV-2 nucleic acid and antibody detection. Chin J Prev Med 2022;56(3):355 – 9. http://dx.doi.org/10.3760/cma.j.cn112150-20211211-01146. (In Chinese).
9. Hoschler K, Ijaz S, Andrews N, Ho S, Dicks S, Jegatheesan K, et al. SARS antibody testing in children: development of oral fluid assays for IgG measurements. Microbiol Spectr 2022;10(1):e0078621. http://dx.doi.org/10.1128/spectrum.00786-21.
10. Heaney CD, Pisanic N, Randad PR, Kruczynski K, Howard T, Zhu XM, et al. Comparative performance of multiplex salivary and commercially available serologic assays to detect SARS-CoV-2 IgG and neutralization titers. medRxiv Preprint. http://dx.doi.org/10.1101/2021.01.28.21250717.
11. George JR, Fitchen JH. Future applications of oral fluid specimen technology. Am J Med 1997;102(4A):21 – 5. http://dx.doi.org/10.1016/s0002-9343(97)00034-x.

Review

Mathematical Models Supporting Control of COVID-19

Bin Deng[1,&]; Yan Niu[2,&]; Jingwen Xu[1]; Jia Rui[1]; Shengnan Lin[1]; Zeyu Zhao[1]; Shanshan Yu[1]; Yichao Guo[1]; Li Luo[1]; Tianmu Chen[1,#]; Qun Li[2,#]

ABSTRACT

Mathematical models have played an important role in the management of the coronavirus disease 2019 (COVID-19) pandemic. The aim of this review is to describe the use of COVID-19 mathematical models, their classification, and the advantages and disadvantages of different types of models. We conducted subject heading searches of PubMed and China National Knowledge Infrastructure with the terms "COVID-19," "Mathematical Statistical Model," "Model," "Modeling," "Agent-based Model," and "Ordinary Differential Equation Model" and classified and analyzed the scientific literature retrieved in the search. We categorized the models as data-driven or mechanism-driven. Data-driven models are mainly used for predicting epidemics, and have the advantage of rapid assessment of disease instances. However, their ability to determine transmission mechanisms is limited. Mechanism-driven models include ordinary differential equation (ODE) and agent-based models. ODE models are used to estimate transmissibility and evaluate impact of interventions. Although ODE models are good at determining pathogen transmission characteristics, they are less suitable for simulation of early epidemic stages and rely heavily on availability of first-hand field data. Agent-based models consider influences of individual differences, but they require large amounts of data and can take a long time to develop fully. Many COVID-19 mathematical modeling studies have been conducted, and these have been used for predicting trends, evaluating interventions, and calculating pathogen transmissibility. Successful infectious disease modeling requires comprehensive considerations of data, applications, and purposes.

INTRODUCTION

Coronavirus disease 2019 (COVID-19) has had a significant impact on public health and economies worldwide (*1*–*2*). Understanding early epidemic trends, providing theoretical support for prevention and control, and evaluating the effect of interventions have been essential foci of COVID-19 research (*3*–*5*). Mathematical models play an important role in the study of transmission mechanisms of infectious diseases; dynamic analyses and model-based predictions help guide selection of interventions (*6*–*9*). However, classification and applications of existing COVID-19 models are not fully described. For example, some researchers use time-series models to predict epidemic trends, while other researchers use stochastic models for the same purpose (*10*–*12*). This situation causes ambiguity in the applicability of models. Classification and applications should be better delineated and standardized, and conditions for appropriate use of specific model types need to be clarified.

For this review we conducted subject heading searches on PubMed and China National Knowledge Infrastructure with search terms "COVID-19," "Mathematical Statistical Model," "Model," "Modeling," "Agent-based Model," and "Ordinary Differential Equation Model." The searches returned 36,021 papers related to mathematical models in the control of COVID-19; 89 met criteria and were included in this review. We reclassified the models described in each paper, summarized their applications to COVID-19, and analyzed advantages and disadvantages of the models to provide a new classification scheme and a selection basis for future modeling research to further promote use of models in COVID-19 prevention and control.

STATUS OF COVID-19 MODELS

We classified mathematical models as either data-driven or mechanism-driven. Data-driven models include time series models, generalized additive models, and artificial neural network (ANN) models, among others. Mechanism-driven models include ordinary differential equation (ODE) and agent-based models. Figure 1 shows our model classification

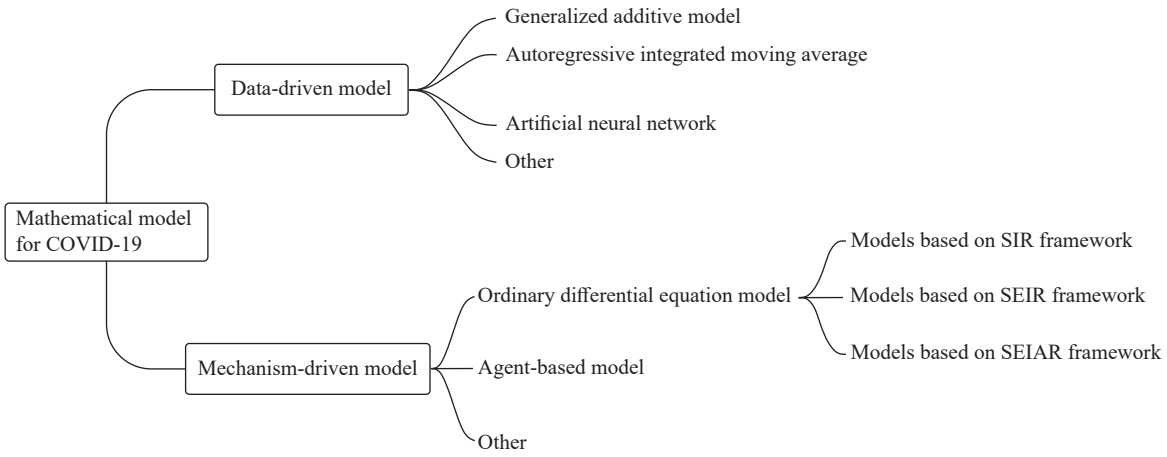

FIGURE 1. Classification of mathematical models in COVID-19.
Abbreviation: COVID-19=coronavirus disease 2019; SIR=susceptible-infectious-removed; SEIR=susceptible-exposed-infectious-removed; SEIAR=susceptible-exposed-infectious-asymptomatic-removed.

scheme. In this review, we focus on data-driven, ODE, and agent-based models.

Data-driven Models

"Data-driven model" is a general term for a collection of models that explore the relationship between instances of diseases and time. These models focus on the relationship between number of infections and time and other factors to predict disease trends. Applications in COVID-19 include growth curve models, generalized logistic growth models (GLM), and other real-time prediction models (*13*–*14*). These models can be used to describe processes of disease development, evaluate uncertainty of disease incidence, and improve the accuracy of trend predictions (*7*). Accuracy can be assessed with indicators such as the Akaike information criterion (AIC), Bayesian information criterion (BIC), and r-squared (R^2).

Autoregressive integrated moving average (ARIMA) models are autoregressive sliding average models based on time-series data. They have been widely used for COVID-19 predictions (*15*–*18*). The basic idea of an ARIMA model is to systematically smooth time-series sampled data to estimate and infer the state of a phenomenon at some future time by revealing the underlying pattern between a target variable and time (*19*). ARIMA models are adaptable and accurate at predicting trends (*20*). We found that for COVID-19 research, ARIMA models focused on comparison of predicted time-series data in different regions.

Artificial neural network models have played an important role in COVID-19 prevention and control research (*19*). ANN models capture uncertainty in time-series data and are a powerful technique for handling nonlinear data, thus complementing traditional linear models and yielding results superior to some other models (*21*–*22*). As a stochastic nonlinear recurrent neural network model, the Boltzmann machine (BM) model is a good fit for analyzing cumulative COVID-19 infection data (*23*–*25*).

Data-driven models have also been used in other scenarios, including prediction and assessment of cumulative deaths prevented in the pandemic (*26*–*27*), optimizing allocation of healthcare resources, and prediction of clinical risk during treatment of COVID-19 (*28*–*30*).

Ordinary Differential Equation Models

ODE models are also known as compartment models (*31*). They reflect the dynamics of infectious diseases based on occurrence and routes of transmission. ODE models reveal epidemiological routes, predict development trends, analyze key factors of disease epidemics, and seek optimal strategies for prevention and control. The most common ODE model is a system of differential equations based on susceptible-infectious-removed (SIR) and susceptible-exposed-infectious-removed (SEIR) compartments (*32*). ODE models can be developed by combining population dynamics, vaccination dynamics, isolation, and population exposures (*33*–*34*).

The basic reproduction number (R_0) is considered a key variable in ODE models that is related to the spread of infectious diseases (*35*–*36*). SIR models have been widely used worldwide, and many studies have

calculated R_0 to help predict COVID-19 trends (*37–40*). SIR models are commonly used to evaluate interventions and calculate transmissibility (*41–42*). The SEIR model has been used to predict and analyze outbreaks (*43–44*). It has also been used to analyze transmission mechanisms in different epidemic scenarios and to predict development of an epidemic (*45–46*). Compared with SIR and SEIR models, the susceptible-exposed-infectious-asymptomatic-removed (SEIAR) model is more applicable for COVID-19 because of its asymptomatic compartment. This model is more suitable for early outbreak predictions (*47–48*). Developing models for different age groups, genders, and occupations helps scholars understand important differences in the spread of COVID-19 under several scenarios (*49*).

Developing effective infectious disease prevention strategies requires consideration of disease characteristics, intervention mechanisms, and resource availability. COVID-19 prevention and control measures include non-pharmaceutical interventions (NPIs) and pharmaceutical interventions (PIs) (*50–54*). NPIs are many, and include isolation, social distancing, wearing masks, and enclosing places of activity (*55*). In our review, we found that nearly 80% of ODE-based research assessed the effects of isolation, doing so by introducing an isolated population into the base-case model and comparing differences in transmission between isolated and non-isolated populations (*11*,*35–56*). Evaluating the effects of other NPIs is achieved by decomposing transmission rate into the probability of transmission of a single contact and the degree of exposure (*57*). For example, wearing a mask reduces the probability of single-contact transmission, whereas increasing social distance reduces the degree of exposure.

An ODE model that incorporated big data on mobile populations was used to simulate changes in epidemic trends in closed and open cities and provide recommendations for policymakers (*58–60*). The most prominent application of ODE models of pharmaceutical interventions is to predict a vaccination campaign's duration, coverage, and impact that will be sufficient to reduce need for NPIs and facilitate recovery of a damaged economy and nation (*61*). Pandemics tend to decrease only gradually after vaccination (*61–62*). Key indicators for vaccination campaigns are vaccine effectiveness and coverage attained, with an inverse relationship between the two indicators, so that higher coverage can partially compensate for lower effectiveness (*61*). Selection of target populations for a vaccination campaign is important. For example, prioritizing vaccination of older age groups is more beneficial for reducing morbidity and mortality (*63–64*).

Agent-based Models

Data-driven and ODE models use population characteristics and do not consider heterogeneity of individuals. Agent-based modeling uses a spatial database of the geographical environment of the study area (*65*) and is usually applied in evaluations of prevention and control measures (*10*,*56–66*). These models can refine studies of interventions, demonstrating, for example, that a combination of testing and close follow-up is more effective than mass testing or self-isolation alone (*67*). Agent-based models makes it possible to evaluate the impact of individual healthcare workers' hand hygiene practices on COVID-19 transmission (*68*). To predict trends in individuals' risk of infection and propose prevention and control strategies, it is necessary to combine individual profiles and demographic data in the model and identify changes in COVID-19 transmission routes in different scenarios (*69–74*). However, data limitations make it difficult to generalize agent-based model results for prediction of COVID-19 trajectory or evaluation of interventions in a city or country.

ADVANTAGES AND DISADVANTAGES OF MODELS

Data-driven Models

Data-driven models have unique advantages in modeling prevention and control of infectious diseases. A wide selection of data-driven models is available, with many featuring ease of use and fast performance for rapid diagnosis in early stages of an outbreak. These models are driven by historical data and statistics and are less affected by parameter changes. However, most data-driven models do not consider natural transmission characteristics and clinical features of the disease. In addition, some key disease parameters lack rigorous interpretation in terms of transmission mechanism or disease etiology, and the models require high-quality historical data, which can challenge assessing effectiveness of some interventions.

Ordinary Differential Equation Models

Compared to agent-based models, ODE models are more flexible, provide more reliable predictions, and

are less computationally demanding. After setting parameters and initial values, ODE models run quickly and are adaptable to the needs of an early and rapid response to a new infectious disease. Additions and deletions can be made according to actual situations, for example, considering different disease states, time-lags, age structures, and birth and death rates. Such adaptations can make the model fit better with reality. The effects of interventions can also be assessed visually by graphing model compartments while changing parameter values. ODE models have some drawbacks. They ignore individual-level heterogeneity and randomness in the disease characteristics; they are not suitable for simulations of epidemics or early cases when some of the parameters are subjective and empirical; and the model results may be realistic and reliable only for the reporting region and may not be generalizable due to regional variability.

Agent-based Models

By using population characteristics and case data and applying mathematical simulation technology to simulate transmission, agent-based models complement epidemiological evaluation of epidemic characteristics and prevention and control measures (*65*). A feature of agent-based models is that the results can reflect spatial and temporal characteristics of a disease in the region, as data-driven and ODE models do. A key advantage is that agent-based models are more useful for analyzing infectious diseases transmission mechanisms and estimating infection rates. Shortcomings include that agent-based individual random models require a large amount of well-measured data and require researchers to have geographic environment modeling experience and a strong foundation in programming.

DISCUSSION

For the COVID-19 pandemic, each type of model has strengths, weaknesses, and a spectrum of applicability to different scientific questions, and each requires varying degrees of background knowledge from the researchers. Infectious disease data-driven models provided information for action by policymakers, clinicians, and public health practitioners during times of great uncertainty about the COVID-19 pandemic. Although most COVID-19 modeling studies used ODE models, as ODE technology advances, future research will involve more cross-pollination between different disciplines. Agent-based models were not widely utilized in COVID-19 prevention and control efforts. Research with more complex and systematic methods has only just begun, and there is still a great deal of in-depth research work to be done in this area.

When dealing with an outbreak of an emerging infectious disease, model selection is based on several points. 1) Stage of the transmission. During the COVID-19 pandemic, different types of models were used at different stages. In the early stages of an epidemic, there is less knowledge about the disease, and therefore only basic SIR or SEIAR models can be built. As the disease is studied and research reveals important insights, it is possible to build more complex models that can perform new and different functions. 2) Data availability. Data are fundamental for building models, and data completeness constrains model selection. When there are insufficient real-world data, researchers can only use basic data-driven models to predict the trajectory of an epidemic. As the amount of data increases and data sources diversify, the type, veracity, and complexity of built models can increase. 3) Applications of the model. When choosing a model, its purpose must be clear. For example, to evaluate the impact of prevention and control measures, one must consider the natural history of the disease, characteristics and settings of the intervention, and other factors. To study the influence of individual factors, an agent-based model should be considered. 4) Generalizability of the model. Most modelling studies are set in small areas, and a model appropriate for one setting may not be applicable elsewhere. Therefore, when selecting model parameters, it is important to consider variability of study sites and parameter values in a comprehensive manner.

Our review has shown that many studies have been conducted with COVID-19 mathematical models, and that mathematical models are highly suitable for analyses of the pandemic. Although many types and applications of COVID-19 models exist, we found that the models can be divided into mechanism-driven models and data-driven models, and that model applications are mainly focused on predicting trends, evaluating the effects of interventions, and estimating severe acute respiratory syndrome coronavirus 2 (SARS-CoV-2) transmissibility. Models are playing a critically important role in COVID-19 prevention and control. In the future, mathematical models will be used to provide scientific support for evidence-based, innovative, and precise responses to many infectious

disease outbreaks.

Conflicts of interest: No conflicts of interest.

Funding: Partly supported by the National Key Research and Development Program of China (2021YFC2301604, 2021ZD0113903).

doi: 10.46234/ccdcw2022.186

[#] Corresponding authors: Tianmu Chen, 13698665@qq.com; Qun Li, liqun@chinacdc.cn.

[1] State Key Laboratory of Molecular Vaccinology and Molecular Diagnostics, School of Public Health, Xiamen University, Xiamen City, Fujian Province, China; [2] Chinese Center for Disease Control and Prevention, Beijing, China.
[&] Joint first authors.

Submitted: September 05, 2022; Accepted: October 03, 2022

REFERENCES

1. Alsharif W, Qurashi A. Effectiveness of COVID-19 diagnosis and management tools: a review. Radiography (Lond) 2021;27(2):682 – 7. http://dx.doi.org/10.1016/j.radi.2020.09.010.
2. Surkova E, Nikolayevskyy V, Drobniewski F. False-positive COVID-19 results: hidden problems and costs. Lancet Respir Med 2020;8 (12):1167 – 8. http://dx.doi.org/10.1016/S2213-2600(20)30453-7.
3. Tang B, Wang X, Li Q, Bragazzi NL, Tang SY, Xiao YN, et al. Estimation of the transmission risk of the 2019-nCoV and its implication for public health interventions. J Clin Med 2020;9(2):462. http://dx.doi.org/10.3390/jcm9020462.
4. Wu JT, Leung K, Leung GM. Nowcasting and forecasting the potential domestic and international spread of the 2019-nCoV outbreak originating in Wuhan, China: a modelling study. Lancet 2020; 395(10225):689 – 97. http://dx.doi.org/10.1016/S0140-6736(20) 30260-9.
5. Yang ZF, Zeng ZQ, Wang K, Wong SS, Liang WH, Zanin M, et al. Modified SEIR and AI prediction of the epidemics trend of COVID-19 in China under public health interventions. J Thorac Dis 2020;12(3):165 – 74. http://dx.doi.org/10.21037/jtd.2020.02.64.
6. Scott N, Palmer A, Delport D, Abeysuriya R, Stuart RM, Kerr CC, et al. Modelling the impact of relaxing COVID-19 control measures during a period of low viral transmission. Med J Aust 2021;214(2):79 – 83. http://dx.doi.org/10.5694/mja2.50845.
7. Roosa K, Lee Y, Luo R, Kirpich A, Rothenberg R, Hyman JM, et al. Real-time forecasts of the COVID-19 epidemic in China from February 5th to February 24th, 2020. Infect Dis Model 2020;5:256 – 63. http://dx.doi.org/10.1016/j.idm.2020.02.002.
8. Attanayake AMCH, Perera SSN, Jayasinghe S. Phenomenological modelling of COVID-19 epidemics in Sri Lanka, Italy, the United States, and Hebei Province of China. Comput Math Methods Med 2020;2020:6397063. http://dx.doi.org/10.1155/2020/6397063.
9. Zou Y, Pan S, Zhao P, Han L, Wang XX, Hemerik L, et al. Outbreak analysis with a logistic growth model shows COVID-19 suppression dynamics in China. PLoS One 2020;15(6):e0235247. http://dx.doi.org/10.1371/journal.pone.0235247.
10. Hoertel N, Blachier M, Blanco C, Olfson M, Massetti M, Rico MS, et al. A stochastic agent-based model of the SARS-CoV-2 epidemic in France. Nat Med 2020;26(9):1417 – 21. http://dx.doi.org/10.1038/s41591-020-1001-6.
11. Koo JR, Cook AR, Park M, Sun YXH, Sun HY, Lim JT, et al. Interventions to mitigate early spread of SARS-CoV-2 in Singapore: a modelling study. Lancet Infect Dis 2020;20(6):678 – 88. http://dx.doi.org/10.1016/S1473-3099(20)30162-6.
12. Lavine JS, Bjornstad ON, Antia R. Immunological characteristics govern the transition of COVID-19 to endemicity. Science 2021;371(6530):741 – 5. http://dx.doi.org/10.1126/science.abe6522.
13. Chowell G, Tariq A, Hyman JM. A novel sub-epidemic modeling framework for short-term forecasting epidemic waves. BMC Med 2019;17(1):164. http://dx.doi.org/10.1186/s12916-019-1406-6.
14. Chowell G, Hincapie-Palacio D, Ospina J, Pell B, Tariq A, Dahal S, et al. Using phenomenological models to characterize transmissibility and forecast patterns and final burden of Zika epidemics. PLoS Curr 20168. http://dx.doi.org/10.1371/currents.outbreaks.f14b2217c902f453d9320a43a35b9583..
15. Liu Q, Li ZQ, Ji Y, Martinez L, Zia UH, Javaid A, et al. Forecasting the seasonality and trend of pulmonary tuberculosis in Jiangsu Province of China using advanced statistical time-series analyses. Infect Drug Resist 2019;12:2311 – 22. http://dx.doi.org/10.2147/IDR.S207809.
16. Dansana D, Kumar R, Das Adhikari J, Mohapatra M, Sharma R, Priyadarshini I, et al. Global forecasting confirmed and fatal cases of COVID-19 outbreak using autoregressive integrated moving average model. Front Public Health 2020;8:580327. http://dx.doi.org/10.3389/fpubh.2020.580327.
17. Duan XD, Zhang XL. ARIMA modelling and forecasting of irregularly patterned COVID-19 outbreaks using Japanese and South Korean data. Data Brief 2020;31:105779. http://dx.doi.org/10.1016/j.dib.2020.105779.
18. Benvenuto D, Giovanetti M, Vassallo L, Angeletti S, Ciccozzi M. Application of the ARIMA model on the COVID-2019 epidemic dataset. Data Brief 2020;29:105340. http://dx.doi.org/10.1016/j.dib.2020.105340.
19. Dhamodharavadhani S, Rathipriya R, Chatterjee JM. COVID-19 mortality rate prediction for India using statistical neural network models. Front Public Health 2020;8:441. http://dx.doi.org/10.3389/fpubh.2020.00441.
20. Wang YD, Yan ZH, Wang D, Yang MT, Li ZQ, Gong XR, et al. Prediction and analysis of COVID-19 daily new cases and cumulative cases: times series forecasting and machine learning models. BMC Infect Dis 2022;22(1):495. http://dx.doi.org/10.1186/s12879-022-07472-6.
21. Namasudra S, Dhamodharavadhani S, Rathipriya R. Nonlinear neural network based forecasting model for predicting COVID-19 cases. Neural Process Lett 2021. https://doi.org/10.1007/S11063-021-10495-W.
22. Naeem M, Yu J, Aamir M, Khan SA, Adeleye O, Khan Z. Comparative analysis of machine learning approaches to analyze and predict the COVID-19 outbreak. PeerJ Comput Sci 2021;7:e746. http://dx.doi.org/10.7717/peerj-cs.746.
23. de Melo GC, de Araújo Neto RA, de Araújo KCGM. Forecasting the rate of cumulative cases of COVID-19 infection in Northeast Brazil: a Boltzmann function-based modeling study. Cad Saude Publica 2020;36(6):e00105720. http://dx.doi.org/10.1590/0102-311x00105720.
24. Fu XM, Ying Q, Zeng TY, Long T, Wang Y. Simulating and forecasting the cumulative confirmed cases of SARS-CoV-2 in China by Boltzmann function-based regression analyses. J Infect 2020;80(5):578 – 606. http://dx.doi.org/10.1016/j.jinf.2020.02.019.
25. Li Q, Feng W, Quan YH. Trend and forecasting of the COVID-19 outbreak in China. J Infect 2020;80(4):469 – 96. http://dx.doi.org/10.1016/j.jinf.2020.02.014.
26. Anastassopoulou C, Russo L, Tsakris A, Siettos C. Data-based analysis, modelling and forecasting of the COVID-19 outbreak. PLoS One 2020;15(3):e0230405. http://dx.doi.org/10.1371/journal.pone.0230405.
27. Xiao LS, Zhang WF, Gong MC, Zhang YP, Chen LY, Zhu HB, et al. Development and validation of the HNC-LL score for predicting the severity of coronavirus disease 2019. eBioMedicine 2020;57:102880. http://dx.doi.org/10.1016/j.ebiom.2020.102880.
28. Liang WH, Liang HR, Ou LM, Chen BF, Chen AL, Li CC, et al. Development and validation of a clinical risk score to predict the occurrence of critical illness in hospitalized patients with COVID-19. JAMA Intern Med 2020;180(8):1081 – 9. http://dx.doi.org/10.1001/jamainternmed.2020.2033.
29. Shahid F, Zameer A, Muneeb M. Predictions for COVID-19 with deep

learning models of LSTM, GRU and Bi-LSTM. Chaos Solitons Fractals 2020;140:110212. http://dx.doi.org/10.1016/j.chaos.2020.110212.
30. Shapiro MB, Karim F, Muscioni G, Augustine AS. Adaptive susceptible-infectious-removed model for continuous estimation of the COVID-19 infection rate and reproduction number in the United States: modeling study. J Med Internet Res 2021;23(4):e24389. http://dx.doi.org/10.2196/24389.
31. Kermack WO, McKendrick AG. Contributions to the mathematical theory of epidemics-I. Bull Math Biol 1991;53(1–2):33 – 55. http://dx.doi.org/10.1016/S0092-8240(05)80040-0.
32. Liu WK, Ye WJ, Zhao ZY, Liu C, Deng B, Luo L, et al. Modelling the emerging COVID-19 epidemic and estimating intervention effectiveness — Taiwan, China, 2021. China CDC Wkly 2021;3(34):716 – 9. http://dx.doi.org/10.46234/ccdcw2021.177.
33. Li KG, Zhao ZY, Wei HJ, Rui J, Huang JF, Guo XH, et al. Feasibility of booster vaccination in high-risk populations for controlling coronavirus variants — China, 2021. China CDC Wkly 2021;3(50):1071 – 4. http://dx.doi.org/10.46234/ccdcw2021.259.
34. Zhao ZY, Niu Y, Luo L, Hu QQ, Yang TL, Chu MJ, et al. The optimal vaccination strategy to control COVID-19: a modeling study in Wuhan City, China. Infect Dis Poverty 2021;10(1):140. http://dx.doi.org/10.1186/s40249-021-00922-4.
35. Hao XJ, Cheng SS, Wu DG, Wu TC, Lin XH, Wang CL. Reconstruction of the full transmission dynamics of COVID-19 in Wuhan. Nature 2020;584(7821):420 – 4. http://dx.doi.org/10.1038/s41586-020-2554-8.
36. Li ZY, Lin SN, Rui J, Bai Y, Deng B, Chen QP, et al. An easy-to-use public health-driven method (the generalized logistic differential equation model) accurately simulated COVID-19 epidemic in Wuhan and correctly determined the early warning time. Front Public Health 2022;10:813860. http://dx.doi.org/10.3389/fpubh.2022.813860.
37. Nguemdjo U, Meno F, Dongfack A, Ventelou B. Simulating the progression of the COVID-19 disease in Cameroon using SIR models. PLoS One 2020;15(8):e0237832. http://dx.doi.org/10.1371/journal.pone.0237832.
38. McMahon A, Robb NC. Reinfection with SARS-CoV-2: discrete SIR (susceptible, infected, recovered) modeling using empirical infection data. JMIR Public Health Surveill 2020;6(4):e21168. http://dx.doi.org/10.2196/21168.
39. Neipel J, Bauermann J, Bo S, Harmon T, Jülicher F. Power-law population heterogeneity governs epidemic waves. PLoS One 2020;15(10):e0239678. http://dx.doi.org/10.1371/journal.pone.0239678.
40. Sharov KS. Trends in adaptation of fifteen European countries population to SARS-CoV-2 in March-May 2020: can Taiwanese experience be adopted? J Formos Med Assoc 2021;120(1):679-87. http://dx.doi.org/10.1016/j.jfma.2020.07.038.
41. Borowiak M, Ning F, Pei J, Zhao S, Tung HR, Durrett R. Controlling the spread of COVID-19 on college campuses. Math Biosci Eng 2020;18(1):551 – 63. http://dx.doi.org/10.3934/mbe.2021030.
42. Anderez DO, Kanjo E, Pogrebna G, Kaiwartya O, Johnson SD, Hunt JA. A COVID-19-based modified epidemiological model and technological approaches to help vulnerable individuals emerge from the lockdown in the UK. Sensors (Basel) 2020;20(17):4967. http://dx.doi.org/10.3390/s20174967.
43. Fan RG, Wang YB, Luo M, Zhang YQ, Zhu CP. SEIR-based COVID-19 transmission model and inflection point prediction analysis. J Univ Electron Sci Technol China 2020;49(3):369-74. https://kns.cnki.net/kcms/detail/detail.aspx?dbcode=CJFD&dbname=CJFDLAST2020&filename=DKDX202003009&uniplatform=NZKPT&v=nYvDwcq-NBNBL28ubxcQm3MRbXiaKSmVHMuxHcs-vFefAzL6ngQ4nUXAFtl060Z7. (In Chinese).
44. Cai J, Jia HY, Wang K. Prediction of development trend of COVID-19 in Wuhan based on SEIR model. Shandong Med J 2020,60(6):1-4. https://kns.cnki.net/kcms/detail/detail.aspx?dbcode=CJFD&dbname=CJFDLAST2020&filename=SDYY202006001&uniplatform=NZKPT&v=8xaANp8M0BwIV90t8tMfOLHObOlIyVZ__8mnxBW2Gk1_DvrEr8BYh7ZyuG5gH_06. (In Chinese).
45. Zhang Y, Tian WL, Wu ZG, Chen ZW, Wang J. Transmission mechanism of COVID-19 epidemic along traffic routes based on improved SEIR model. J Traffic Transp Eng 2020;20(3):150 – 8. http://dx.doi.org/10.19818/j.cnki.1671-1637.2020.03.014. (In Chinese).
46. Ahmad Z, Arif M, Ali F, Khan I, Nisar KS. A report on COVID-19 epidemic in Pakistan using SEIR fractional model. Sci Rep 2020;10(1):22268. http://dx.doi.org/10.1038/s41598-020-79405-9.
47. Niu Y, Rui J, Wang QP, Zhang W, Chen ZW, Xie F, et al. Containing the transmission of COVID-19: a modeling study in 160 countries. Front Med (Lausanne) 2021;8:701836. http://dx.doi.org/10.3389/fmed.2021.701836.
48. Zhao ZY, Zhu YZ, Xu JW, Hu SX, Hu QQ, Lei Z, et al. A five-compartment model of age-specific transmissibility of SARS-CoV-2. Infect Dis Poverty 2020;9(1):117. http://dx.doi.org/10.1186/s40249-020-00735-x.
49. Chen TM, Zhao ZY, Rui J, Yu SS, Zhu YZ, Xu JW, et al. Estimating the transmissibility of coronavirus disease 2019 and assessing the effectiveness of the countermeasures to control the disease in Xiamen City. J Xiamen Univ (Nat Sci) 2020;59(3):298-303. https://kns.cnki.net/kcms/detail/detail.aspx?dbcode=CJFD&dbname=CJFDLAST2020&filename=XDZK202003002&uniplatform=NZKPT&v=zviJ1kZOe2jhn9QwSusdNIs_Q5A03drMNkbR5XqbESvnBaRDkvIBuTPfU2Iyq6rf. (In Chinese).
50. Leung CC, Lam TH, Cheng KK. Mass masking in the COVID-19 epidemic: people need guidance. Lancet 2020;395(10228):945. http://dx.doi.org/10.1016/S0140-6736(20)30520-1.
51. Hens N, Vranck P, Molenberghs G. The COVID-19 epidemic, its mortality, and the role of non-pharmaceutical interventions. Eur Heart J Acute Cardiovasc Care 2020;9(3):204 – 8. http://dx.doi.org/10.1177/2048872620924922.
52. Flaxman S, Mishra S, Gandy A, Unwin HJT, Mellan TA, Coupland H, et al. Estimating the effects of non-pharmaceutical interventions on COVID-19 in Europe. Nature 2020;584(7820):257 – 61. http://dx.doi.org/10.1038/s41586-020-2405-7.
53. Liu PJ, Rahman MU, Din A. Fractal fractional based transmission dynamics of COVID-19 epidemic model. Comput Methods Biomech Biomed Engin 20221 – 18. http://dx.doi.org/10.1080/10255842.2022.2040489..
54. Lin SN, Rui J, Chen QP, Zhao B, Yu SS, Li ZY, et al. Effectiveness of potential antiviral treatments in COVID-19 transmission control: a modelling study. Infect Dis Poverty 2021;10(1):53. http://dx.doi.org/10.1186/s40249-021-00835-2.
55. Ngonghala CN, Iboi E, Eikenberry S, Scotch M, MacIntyre CR, Bonds MH, et al. Mathematical assessment of the impact of non-pharmaceutical interventions on curtailing the 2019 novel Coronavirus. Math Biosci 2020;325:108364. http://dx.doi.org/10.1016/j.mbs.2020.108364.
56. Kucharski AJ, Klepac P, Conlan AJK, Kissler SM, Tang ML, Fry H, et al. Effectiveness of isolation, testing, contact tracing, and physical distancing on reducing transmission of SARS-CoV-2 in different settings: a mathematical modelling study. Lancet Infect Dis 2020;20(10):1151 – 60. http://dx.doi.org/10.1016/S1473-3099(20)30457-6.
57. Hachtel GD, Stack JD, Hachtel JA. Forecasting and modeling of the COVID-19 pandemic in the USA with a timed intervention model. Sci Rep 2022;12(1):4339. http://dx.doi.org/10.1038/s41598-022-07487-8.
58. Eikenberry SE, Mancuso M, Iboi E, Phan T, Eikenberry K, Kuang Y, et al. To mask or not to mask: modeling the potential for face mask use by the general public to curtail the COVID-19 pandemic. Infect Dis Model 2020;5:293 – 308. http://dx.doi.org/10.1016/j.idm.2020.04.001.
59. Iboi EA, Sharomi O, Ngonghala CN, Gumel AB. Mathematical modeling and analysis of COVID-19 pandemic in Nigeria. Math Biosci Eng 2020;17(6):7192 – 220. http://dx.doi.org/10.3934/mbe.2020369.
60. Shen MW, Zu J, Fairley CK, Pagán JA, Ferket B, Liu B, et al. Effects of New York's executive order on face mask use on COVID-19 infections and mortality: a modeling study. J Urban Health 2021;98(2):197 – 204. http://dx.doi.org/10.1007/s11524-021-00517-2.

61. Keeling MJ, Hill EM, Gorsich EE, Penman B, Guyver-Fletcher G, Holmes A, et al. Predictions of COVID-19 dynamics in the UK: short-term forecasting and analysis of potential exit strategies. PLoS Comput Biol 2021;17(1):e1008619. http://dx.doi.org/10.1371/journal.pcbi.1008619.
62. Suthar DL, Habenom H, Aychluh M. Effect of vaccination on the transmission dynamics of COVID-19 in Ethiopia. Results Phys 2022;32:105022. http://dx.doi.org/10.1016/j.rinp.2021.105022.
63. Shen MW, Zu J, Fairley CK, Pagán JA, An L, Du ZW, et al. Projected COVID-19 epidemic in the United States in the context of the effectiveness of a potential vaccine and implications for social distancing and face mask use. Vaccine 2021;39(16):2295 – 302. http://dx.doi.org/10.1016/j.vaccine.2021.02.056.
64. Li YX, Ge LQ, Zhou Y, Cao X, Zheng JY. Toward the impact of non-pharmaceutical interventions and vaccination on the COVID-19 pandemic with time-dependent SEIR model. Front Artif Intell 2021;4:648579. http://dx.doi.org/10.3389/frai.2021.648579.
65. Laubenbacher R, Hinkelmann F, Oremland M. Chapter 5 - Agent-based models and optimal control in biology: a discrete approach. In: Robeva R, Hodge TL, editors. Mathematical concepts and methods in modern biology. Amsterdam: Academic Press. 2013143 – 78. http://dx.doi.org/10.1016/B978-0-12-415780-4.00005-3.
66. Hoertel N, Blachier M, Blanco C, Olfson M, Massetti M, Rico MS, et al. Lockdown exit strategies and risk of a second epidemic peak: a stochastic agent-based model of SARS-CoV-2 epidemic in France. medRxiv 2020. http://dx.doi.org/10.1101/2020.04.30.20086264.
67. Mahdizadeh Gharakhanlou N, Hooshangi N. Spatio-temporal simulation of the novel coronavirus (COVID-19) outbreak using the agent-based modeling approach (case study: Urmia, Iran). Inform Med Unlocked 2020;20:100403. http://dx.doi.org/10.1016/j.imu.2020.100403.
68. Nguyen LKN, Howick S, McLafferty D, Anderson GH, Pravinkumar SJ, Van Der Meer R, et al. Evaluating intervention strategies in controlling coronavirus disease 2019 (COVID-19) spread in care homes: an agent-based model. Infect Control Hosp Epidemiol 2021;42(9):1060 – 70. http://dx.doi.org/10.1017/ice.2020.1369.
69. Cuevas E. An agent-based model to evaluate the COVID-19 transmission risks in facilities. Comput Biol Med 2020;121:103827. http://dx.doi.org/10.1016/j.compbiomed.2020.103827.
70. Rockett RJ, Arnott A, Lam C, Sadsad R, Timms V, Gray KA, et al. Revealing COVID-19 transmission in Australia by SARS-CoV-2 genome sequencing and agent-based modeling. Nat Med 2020;26(9):1398 – 404. http://dx.doi.org/10.1038/s41591-020-1000-7.
71. Ying FB, O'Clery N. Modelling COVID-19 transmission in supermarkets using an agent-based model. PLoS One 2021;16(4):e0249821. http://dx.doi.org/10.1371/JOURNAL.PONE.0249821.
72. Araya F. Modeling the spread of COVID-19 on construction workers: an agent-based approach. Saf Sci 2021;133:105022. http://dx.doi.org/10.1016/j.ssci.2020.105022.
73. Lombardo G, Pellegrino M, Tomaiuolo M, Cagnoni S, Mordonini M, Giacobini M, et al. Fine-grained agent-based modeling to predict COVID-19 spreading and effect of policies in large-scale scenarios. IEEE J Biomed Health Inform 2022;26(5):2052 – 62. http://dx.doi.org/10.1109/JBHI.2022.3160243.
74. Thompson J, McClure R, Blakely T, Wilson N, Baker MG, Wijnands JS, et al. Modelling SARS-CoV-2 disease progression in Australia and New Zealand: an account of an agent-based approach to support public health decision-making. Aust N Z J Public Health 2022;46(3):292 – 303. http://dx.doi.org/10.1111/1753-6405.13221.

Notes from the Field

First Imported Case of SARS-CoV-2 Omicron Subvariant BA.4 — Guangdong Province, China, May 4, 2022

Qianfang Guo[1,&]; Changcheng Wu[2,&]; Aiping Deng[1]; Jingtao Liang[3]; Xiang Zhao[2]; Ruhan A[2]; Jiajun Liu[1]; Fangzhu Ouyang[1]; Jing Xu[1]; Shen Huang[1]; Yang Song[2]; Lirong Zou[1]; Xiaoling Deng[1]; Kai Nie[2,#]; Baisheng Li[1,#]

On April 29, 2022, a flight arrived at Baiyun International Airport, Guangzhou City, Guangdong Province, after departing from Amsterdam Schiphol Airport, the Netherlands. After the first test of severe acute respiratory syndrome coronavirus 2 (SARS-CoV-2) nucleic acid at the Baiyun International Airport, all passengers were admitted to a quarantine hotel for a routine 14-day medical observation. On April 30, one of the passengers (a 20-year-old Chinese female) was reported positive for coronavirus disease 2019 (COVID-19), and then a nasopharyngeal swab sample was immediately retested on May 1 and reported positive. The patient was fully vaccinated against COVID-19 and completed 14 days of quarantine before flying to China. She denied any history of exposure to COVID-19 cases. After diagnosis, the patient was sent to Foshan Fourth People's Hospital for treatment.

On May 4, 2022, the viral genomic sequence of the patient was obtained using the Illumina MiniSeq platform (Illumina, San Diego, CA, USA), and genotyping results showed that the genome belonged to the Omicron/variant of concern (VOC) sublineage BA.4, with a total of 30 amino acid mutations (V3G, T19I, A27S, G142D, V213G, G339D, S371F, S373P, S375F, T376A, D405N, R408S, K417N, N440K, L452R, S477N, T478K, E484A, F486V, Q498R, N501Y, Y505H, D614G, H655Y, N679K, P681H, N764K, D796Y, Q954H, N969K) and 5 deletions (L24del, P25del, P26del, H69del, V70del) in the spike protein gene. The phylogenetic tree indicates that the sequenced BA.4 has high similarity to the genome detected in Denmark on May 4, 2022 (GISAID: EPI_ISL_12648960) (Figure 1). The sequence has been deposited in the National Genomics Data Center (under the accession number WGS025540).

On May 4, 2022, the World Health Organization reminded to closely monitor Omicron BA.4 subvariants (*1*). BA.4 is driving the upsurge in South Africa and has rapidly replaced BA.2, with over 50% of sequenced cases since the first week of April 2022 (*2*). Compared to BA.2, the BA.4 subvariants also showed stronger immune escape to the plasma of 3-dose vaccinees, even vaccinated BA.1 convalescent plasma (*3–4*). Cases of BA.4 infection have been reported in at least 20 countries, mainly from South Africa (62.39%) (*5–6*). Researchers are focusing on this subvariant and trying to learn more.

doi: 10.46234/ccdcw2022.095

Corresponding authors: Kai Nie, niekai@ivdc.chinacdc.cn; Baisheng Li, libsn@126.com.

[1] Guangdong Provincial Center for Disease Control and Prevention, Guangzhou City, Guangdong Province, China; [2] National Institute for Viral Disease Control and Prevention, Chinese Center for Disease Control and Prevention, Beijing, China; [3] Foshan Center for Disease Control and Prevention, Foshan City, Guangdong Province, China.
[&] Joint first authors.

Submitted: May 16, 2022; Accepted: May 18, 2022

REFERENCES

1. World Health Organization. COVID-19 weekly epidemiological update edition 90, published 4 May 2022. https://apps.who.int/iris/bitstream/handle/10665/353976/nCoV-weekly-sitrep4May22-eng.pdf?sequence=1&isAllowed=y. [2022-5-5].
2. Tegally H, Moir M, Everatt J, Giovanetti M, Scheepers C, Wilkinson E, et al. Continued Emergence and Evolution of Omicron in South Africa: New BA.4 and BA.5 lineages. medRxiv 2022. http://dx.doi.org/10.1101/2022.05.01.22274406.
3. Khan K, Karim F, Ganga Y, Bernstein M, Jule Z, Reedoy K, et al. Omicron sub-lineages BA.4/BA.5 escape BA.1 infection elicited neutralizing immunity. medRxiv 2022. http://dx.doi.org/10.1101/2022.04.29.22274477.
4. Cao Y, Yisimayi A, Jian F, Song W, Xiao T, Wang L, et al. BA2.12.1, BA.4 and BA.5 escape antibodies elicited by Omicron infection. bioRxiv 2022. http://dx.doi.org/10.1101/2022.04.30.489997.
5. Outbreak.info. Lineage | Mutation Tracker: BA.4 Lineage Report. https://outbreak.info/situation-reports?pango=BA.4. [2022-5-8].
6. GASAID. hCoV-19 tracking of variants (menu option BA.4). https://www.gisaid.org/hcov19-variants/. [2022-5-8].

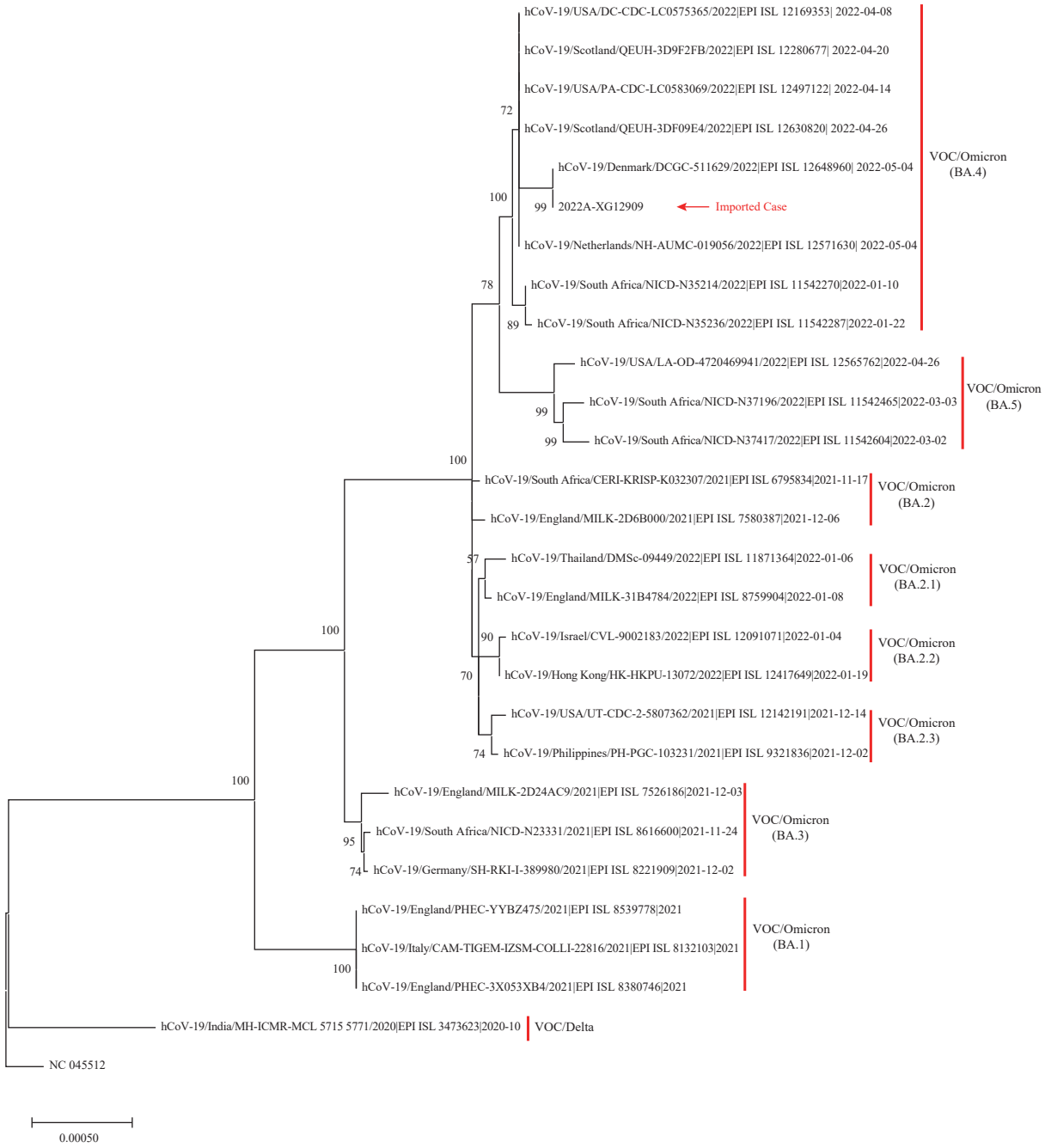

FIGURE 1. Phylogenetic tree based on the full-length genome sequences of the COVID-19 Omicron sublineage.
Note: The Guangdong Province imported VOC/Omicron (BA.4) variant is indicated with a red arrow. The other Omicron sublineages are indicated on the right side and marked with vertical bars.
Abbreviation: COVID-19=coronavirus disease 2019; VOC=variant of concern.

Notes from the Field

Emergence of a SARS-CoV-2 Omicron Subvariant BA.2.2 with a 454-Nucleotide Genomic Deletion — Sichuan Province, China, May 10, 2022

Yuliang Feng[1,&]; Xiang Zhao[2,&]; Tao Luo[3,&]; Zhixiao Chen[2]; Huiping Yang[1]; Na Chen[1]; Xiaozhen Ma[1]; Mingyuan Li[3]; Weihua Zhang[4]; Sikai Jia[3]; Xun Yuan[5]; Ming Pan[1,#]; Linlin Zhou[3,#]

On May 9, 2022, 3 local residents in Guang'an City, Sichuan Province, tested positive for severe acute respiratory syndrome coronavirus 2 (SARS-CoV-2) and were diagnosed with asymptomatic coronavirus disease 2019 (COVID-19) in a local outbreak, and as of May 14, a total of 20 confirmed cases and 398 asymptomatic infections were reported.

Whole genome sequencing was performed directly on the nasal and throat swab specimens from the initial three asymptomatic infected individuals using the Illumina MiSeq platform (Illumina, San Diego, CA, USA). The complete genome sequences of 3 SARS-CoV-2 strains, named SC1215, SC1216, and SC1217, were obtained. The sequence of SC1217 has been deposited in the GISAID database (under the accession number EPI_ISL_12725020). Phylogenetic analysis (maximum likelihood method) revealed that the 3 local strains clustered together to form a monophyletic clade belonging to the Omicron BA.2.2 sublineage (Figure 1) (*1*–*2*). The BA.2.2 sublineage was derived from the Omicron BA.2 lineage (*3*) and may have originated in Hong Kong Special Administrative Region (SAR) with predominant transmission to the mainland of China, Japan, Australia, and the United Kingdom (*2*).

Genomic analysis revealed a 454 nucleotide (nt) deletion in the SARS-COV-2 genome at nucleotide positions 27,689–28,142, and this result was further validated by Sanger sequencing (Figure 2). Sequencing of 41 clinical specimens from the local outbreak in Guang'an by May 14 had also detected the 454-nt deletion. Further analysis revealed that the 454-nt deletion resulted in a 71-nt deletion at the 3' end of ORF7a gene, a complete deletion of ORF7b gene (132-nt) and the intergenic region of ORF7b/8 (6-nt) gene, and a 249-nt deletion at the 5' end of ORF8 gene.

As of May 12, 2022, 2,787 sequences in the GISAID database were Omicron BA.2.2 sublineage, but no such long 454-nt deletion was found. ORF7a, ORF7b, and ORF8, which encode accessory proteins of SARS-CoV-2, are important for the interaction of SARS-CoV-2 with the host. Previous studies have shown that ORF7a protein binds to human monocytes, decreases antigen presentation ability, and induces dramatic expression of pro-inflammatory cytokines (*4*–*5*). Deletion of ORF8 may lead to a milder infection and a more efficient immune response to SARS-CoV-2 (*6*). Further experiments are needed on whether and how this 454-nt deletion affects the infectivity and pathogenicity of the virus, and epidemiological and genomic surveillance is needed to monitor its potential further transmission.

Funding: Sichuan Science and Technology Program (2022ZDZX0017 and 2021YFQ0060).

doi: 10.46234/ccdcw2022.098

Corresponding authors: Ming Pan, panming1983@sina.com; Linlin Zhou, zhoulinlin@scu.edu.cn.

[1] Sichuan Center for Disease Control and Prevention, Chengdu City, Sichuan Province, China; [2] National Institute for Viral Disease Control and Prevention, Chinese Center for Disease Control and Prevention, Beijing, China; [3] West China School of Basic Medical Sciences & Forensic Medicine, Sichuan University, Chengdu City, Sichuan Province, China; [4] College of Computer Science, Sichuan University, Chengdu City, Sichuan Province, China; [5] Guang'an Center for Disease Control and Prevention, Guang'an City, Sichuan Province, China.

& Joint first authors.

Submitted: May 17, 2022; Accepted: May 20, 2022

REFERENCES

1. World Health Organization. Weekly epidemiological update on COVID-19 - 30 November 2021. 2021. https://www.who.int/publications/m/item/weekly-epidemiological-update-on-covid-19---30-november-2021. [2022-5-15].
2. GitHub. BA.2 sub-lineage with S:I1221T dominant in Hong Kong #430. 2022. https://github.com/cov-lineages/pango-designation/issues/430. [2022-5-15].
3. GitHub. Proposal to split B.1.1.529 to incorporate a newly characterised sibling lineage #361. 2021. https://github.com/cov-lineages/pango-designation/issues/361. [2022-5-15].
4. Panzera Y, Ramos N, Frabasile S, Calleros L, Marandino A, Tomás G,

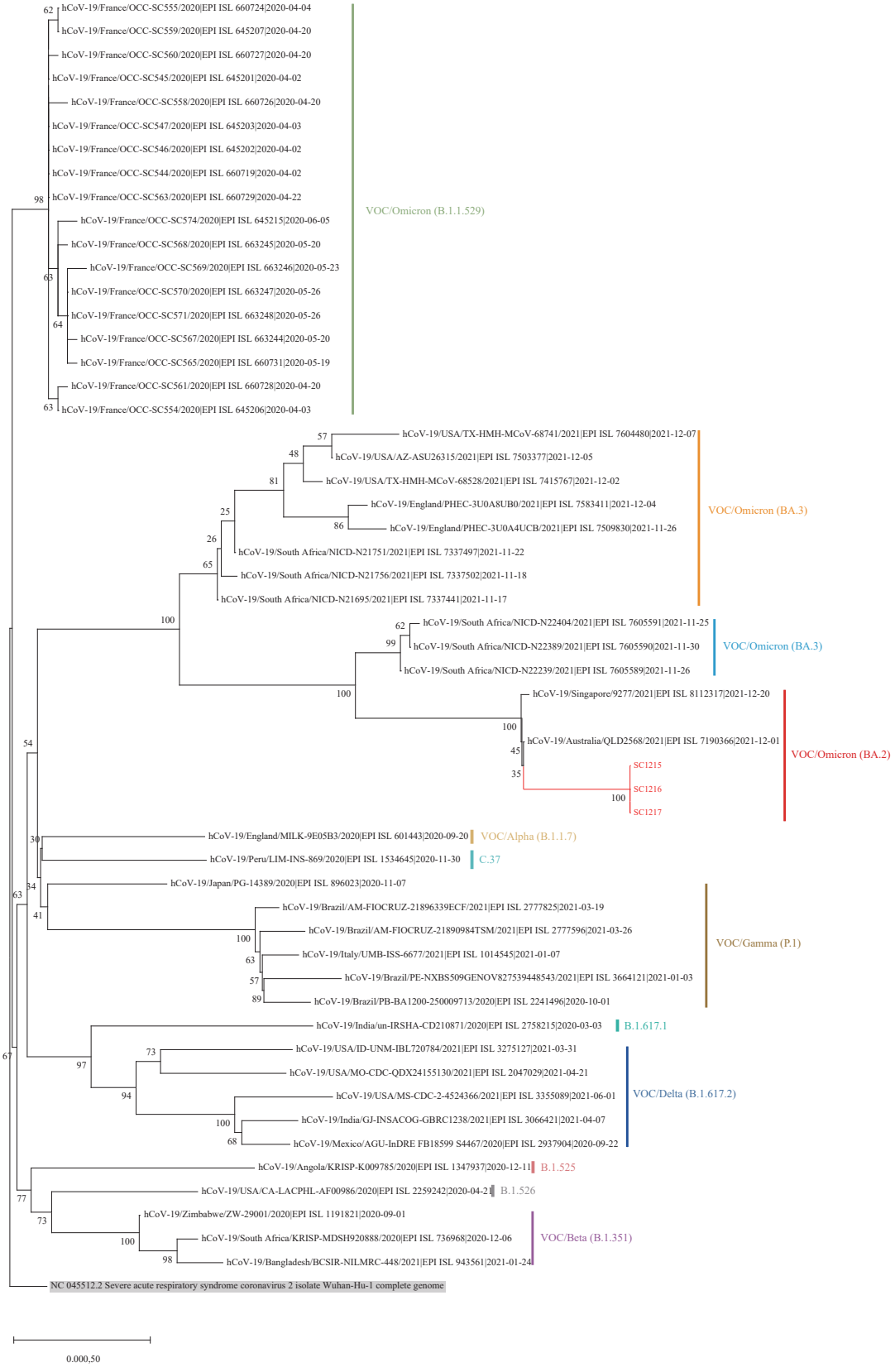

FIGURE 1. The maximum likelihood phylogeny based on the full-length genome sequences of SARS-CoV-2.
Note: The Sichuan 454-nt deletion variants are highlighted in red. The Wuhan reference strain is shaded in gray.
Abbreviation: VOC=variant of concern; SARS-CoV-2=severe acute respiratory syndrome coronavirus 2.

FIGURE 2. Genomic organization of human SARS-CoV-2 and the location of the 454-nt deletion(Δ454). (A) Schematic diagram of the genomes of SARS-CoV-2 isolates Wuhan-Hu-1 (Genbank: NC_045512, GISAID: EPI_ISL_402125). (B) Magnification of genomic region (red box in panel A) showing the 454-nt deletion spanning ORF7a, ORF7b, and ORF8 (indicated by the red line). (C) Sanger sequencing results flanking the 454-nt deletion of the SARS-CoV-2 Δ454 variant.
Abbreviation: SARS-CoV-2=severe acute respiratory syndrome coronavirus 2.

et al. A deletion in SARS‐CoV‐2 ORF7 identified in COVID-19 outbreak in Uruguay. Transbound Emerg Dis 2021;68(6):3075 – 82. http://dx.doi.org/10.1111/tbed.14002.

5. Zhou ZL, Huang CL, Zhou ZC, Huang ZX, Su LL, Kang SS, et al. Structural insight reveals SARS-CoV-2 Orf7a as an immunomodulating factor for human CD14+monocytes. iScience 2021;24(3):102187. http://dx.doi.org/10.1016/j.isci.2021.102187.

6. Young BE, Fong SW, Chan YH, Mak TM, Ang LW, Anderson DE, et al. Effects of a major deletion in the SARS-CoV-2 genome on the severity of infection and the inflammatory response: an observational cohort study. Lancet 2020;396(10251):603 – 11. http://dx.doi.org/10.1016/S0140-6736(20)31757-8.

Indexed by PubMed Central (PMC), Emerging Sources Citation Index (ESCI), Scopus, Chinese Scientific and Technical Papers and Citations, and Chinese Science Citation Database (CSCD)

The inauguration of *China CDC Weekly* is in part supported by Project for Enhancing International Impact of China STM Journals Category D (PIIJ2-D-04-(2018)) of China Association for Science and Technology (CAST).

CCDC weekly

Vol. 4 No. 40 Oct. 7, 2022

Responsible Authority
National Health Commission of the People's Republic of China

Sponsor
Chinese Center for Disease Control and Prevention

Editing and Publishing
China CDC Weekly Editorial Office
No.155 Changbai Road, Changping District, Beijing, China
Tel: 86-10-63150501, 63150701
Email: weekly@chinacdc.cn

CSSN
ISSN 2096-7071
CN 10-1629/R1